Modelling Rhizomania in Sugar Beet

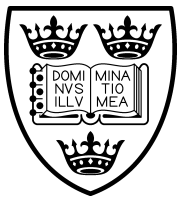

T. Déirdre Hollingsworth

Lincoln College

University of Oxford

Dissertation submitted as a partial
requirement for the degree of

Master of Science
Mathematical Modelling and Numerical Analysis

September 1999

With love and gratitude to my parents, for all their advice and encouragement.

Acknowledgements

I would like to express my sincere gratitude to Dr. Fowler, for his help and guidance as my supervisor for this dissertation. I would also like to thank Dr. Howison for his support as my supervisor during the earlier part of the year, and Dr. Gilligan and Dr. Truscott for the invaluable discussions.

I would like to thank the OCIAM Industrial Fund for funding me this year, and Lincoln College for the delicious food and comfortable accommodation.

My thanks go to Keith Gillow, who has always been helpful with queries about LaTeX, and all the staff in the Mathematical Institute and Computing Laboratory.

I am very grateful to my parents and brother for their continuing guidance and support. I am also indebted to those who have made this year so enjoyable. In particular I would like to thank Ben, for all his help and encouragement, and Caroline, for the lunches at St. Cross and the great chats.

Contents

Chapter 1

Introduction

In this dissertation, we shall study a model of the disease *rhizomania* in sugar beet. This is a fungal root disease with primary and secondary infection mechanisms. The disease is regularly interrupted by harvesting and sowing. The aim of the mathematical model is to understand the dynamics of the disease, and eventually to suggest a way to map the disease from one year to the next. The effect of temperature on the level of infection is also studied. Some of the biological terms, which are italicised, are explained in the glossary.

Sugar beet, or *beta vulgaris*, is a biennial herb, grown from seed. It is grown for the sugar in its swollen root, and harvested at the end of the first year. Sugar beets have white roots of conical shape, growing deep into the soil (about 1 m) with only the crown exposed, as seen in Figure 1.1. The first sugar beet factory was opened in Prussia in 1801, with sugar yields of about 4% of root body weight. This yield has been increased, by selection and breeding, to a maximum of about 20%. A typical statistic would be about 40 tonnes of root per hectare, producing $6-7$ tonnes of sugar. Sugar beet is now grown all over the world, from Greece to Japan. The sugar content is highest in areas with cool temperatures, good sunlight and with well-drained soil. Sugar beet is responsible for 40% of the world's sugar supply, and is second only to sugar cane. In the northern hemisphere, sugar beets are generally planted in the spring and harvested in the autumn.

Rhizomania is a disease which significantly affects the yield of sugar beet, and thus is of great concern to sugar producers. The first major case of rhizomania is believed to have occurred in Italy in 1952 [1], where there were reports of very poor yields and symptoms similar to those of rhizomania, which are described in Section 1.1.1. Cultivation in some areas had to be abandoned because of the decline in yield. The disease was named 'rhizomania', or 'root madness', by Canova in 1966, after one of its symptoms. Canova was the first to identify the cause of the infection as an association between a virus and a fungus, *Polymyxa betae*, found in the affected roots. It is the persistence and proliferation of this fungal vector which is responsible for the

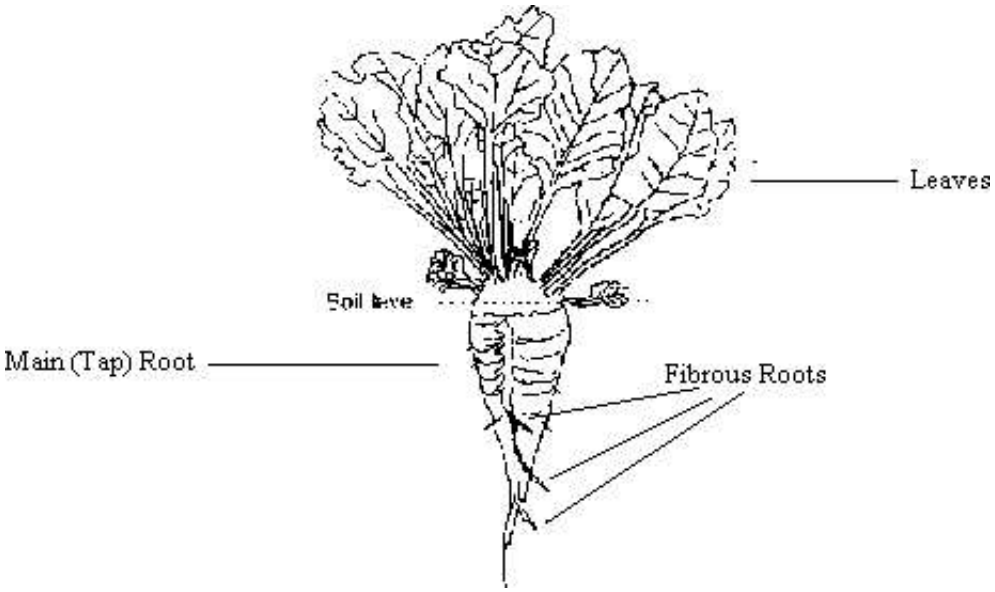

Figure 1.1: Diagram of a sugar beet. The main, tap root, lies almost completely below soil level, and is surrounded by lateral, or fibrous roots. Reproduced from [1].

development and spread of rhizomania. The action of these agents is discussed below. Some of the information used below comes from the web pages of British Sugar [15]; University of Ohio Plant Biology Department, Plasmodiophorid Home Page [12] and IACR-Broom's Barn, Sugar Beet [2].

Intensive research in the late 1960s, motivated by numerous cases of rhizomania in Japan in 1965, led to the isolation of the viral agent, beet necrotic yellow vein virus or BNYVV. The widespread nature of the infection in Japan was attributed to the practice of transplanting seedlings to establish a sugar beet crop, which meant that infected soil used to raise a batch of seedlings could infect large areas.

Rhizomania was found across Europe in the 1970s, when a test for the disease was devised. There were no cases in Eire or Scandinavia in 1993, even though the fungus was believed to be present in the soil. Asher [1] suggests that this may reflect poor opportunities for infection due to cooler climates than the rest of Europe.

1.1 Rhizomania

1.1.1 Symptoms of Rhizomania

The beet necrotic yellow vein virus was named after one of the classical symptoms of the infection, the veins in the leaves becoming yellow, then brown. The patches of yellow leaves in an infected field are shown in Figure 1.2. This symptom only develops when the infection becomes systemic, which occurs infrequently. A more common symptom is the distortion of the main, or tap, root, as seen in Figure 1.3.

Figure 1.2: A rhizomania infected field in the Netherlands, with yellow patches of leaves. Reproduced from [3].

If a plant is infected at an early stage in its development, the tap root becomes very long and thin, yellow or green in colour, with a proliferation of lateral roots, called the 'beard'. It is within this beard that the fungus and virus proliferate. The leaves may be pale green with a longer shape. These symptoms are less dramatic in a plant that is infected at a later stage in its development. It appears that as the plants grow older, they become resistant to the disease.

Yield losses due to rhizomania, which can be in the region of 60%, depend on how much each tap root has been constricted, and thus whether the crop is infected at an early stage of its development. This is directly related to the amount of infectious material in the soil at the beginning of the season.

1.1.2 Causes of Infection

Beet necrotic yellow vein virus is a complex, fungally transmitted, rod shaped virus. The rod shaped particles are about 20 nm wide and of varying length, from about 85 to 390 nm. This virus is carried by the fungus *Polymyxa betae*, which was first identified by Keskin in 1964 [11]. *Polymyxa betae* is an *obligate parasite* which spreads and infects using *zoospores*, not filamentous hyphae, as most fungi do.

Figure 1.3: Cross-section of a diseased sugar beet The tap root is constricted and necrotic. Reproduced from [3].

The initial infection is by motile biflagellate zoospores, of about 5μm in diameter, which infect a root hair, or epidermal cell. They appear to be attracted to the site of infection, but there is no clear evidence of this. The zoospores remain attached to the host cell while they form a cyst, lose their *flagella*, and form a dagger-like body, or *stachel*, within the cyst. The stachel is then used to penetrate the cell wall, allowing the contents of the cyst to pass into the host cell. The virus is thus introduced into the host. This process is represented diagrammatically in Figure 1.4. Infection of a seedling root can occur in under ten minutes in a zoospore suspension [13].

It has been observed [3] that infection of young cells is far more common than that of older cells. The zoospores probe the cells with the pointed end of their flagella until a suitable cell is selected. It is possible that this preferential infection of young cells is in response to a chemotactic stimulus exuding from these cells, or that the older cells have thicker walls due to deposits. The largest quantity of new root hairs is produced near the tips of the fibrous roots, and it is here that the infection proliferates.

Once the fungus is inside the host cell, it develops into a *sporangial plasmodium*, filling the cell volume, perhaps sharing it with at least one other plasmodium from

independent infections. These plasmodia differentiate into zoosporangia containing a variable number of secondary zoospores. The secondary zoospores are released from the host by means of an exit tube. They swim through the soil and infect other roots and neighbouring plants, actively spreading the disease. This cycle is repeated with each new infection, leading to the rapid spread of the disease through a growing season.

As the season progresses, more zoospores preferentially form cystogenous plasmodia, rather than sporangial plasmodia. The reason for this change is not known. It is possible that it is a response to the high density of infection among the roots of an infected plant, or the onset of the sexual cycle in the parasite. The cystogenous plasmodia eventually form into mature resting spores, or *cystori*. These may consist of as few as four or as many as three hundred hexagonal or polyhedra walled cysts, of variable size, between 4 and 7μm in diameter. There may be several of these cystori in a single plant cell. They are released into the soil when the fibrous roots are removed from the tap root, which occurs at harvest. The cystori can survive in the soil intact for up to fifteen or twenty years. This longevity is believed to be due to the make up of the spore wall, although this is yet to be determined.

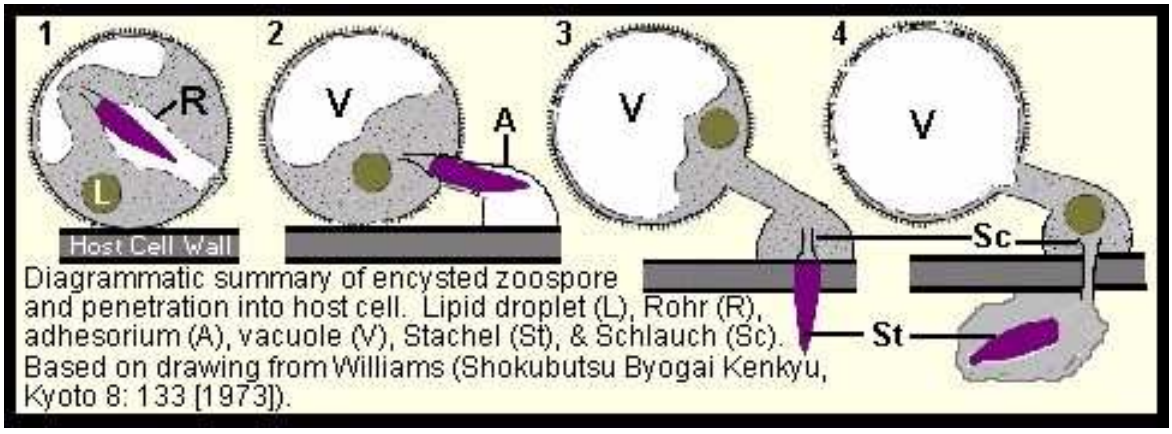

Figure 1.4: Diagrammatic representation of penetration of the host cell by the encysted zoospore. Reproduced from [12].

When these cysts germinate they release zoospores into the soil, thus beginning the life cycle again. It is not known what causes the cyst to germinate, with different cysts from a single resting spore germinating at different times in identical conditions. A cyst was even found to germinate in distilled water. Germination is believed to occur when the soil temperature is over 10-15°C [1]. The optimum temperature is 25°C [4], as is that for virus synthesis [1]. This would suggest that rhizomania should be more widespread and infections more severe in countries with warm temperatures in the spring and early summer, when the roots are most vulnerable. This is generally true, for example in Mediterranean or California, where soil temperatures may be as high as 20°C when the sugar beets are sown.

This relation between soil temperature and levels of infection can be exploited to reduce levels of infection, or to reduce the amount of damage to crops in fields which are already infested with rhizomania. If seedings are raised in sterilised soil in paper plots, before being mechanically transplanted into the soil, the time at which the plants become infected is delayed. This transplanting method significantly increases sugar yields, as reported in Richard-Molard [14], but is expensive. It is economically viable in Japan, where it is used routinely.

The benefits of developing the plants before the infection can begin may be obtained by early planting in some countries. Since sugar beet can grow at temperatures as low as three degrees centigrade, the beet can grow unaffected by rhizomania until the temperature rises to about ten degrees. Trials of this method led to a forty-five percent increase in sugar yield in an infected field in Germany.

The cysts also require water to germinate, and for the zoospores to swim through the soil to the roots. The amount of water required is different for every type of soil, but there have been some studies where a limiting matric potential of greater than 400 mbars was required [6]. As the amount of soil moisture is increased, the activity of the fungus is increased, and hence so is the level and range of infection. Irrigated fields, or low-lying fields, with a higher water table, have been found to have high levels of infection. Thus, if the levels of soil moisture are reduced, this can lower the levels of infection. This can be achieved by maintaining good soil structure and drainage.

The acidity of the soil is also a factor in the level of infection, with neutral or alkaline soils having more severe infection. High levels of rapid infection are seen in experiments with soil at pH $6-8$. Cystori cannot germinate at a pH lower than 5, but can remain viable, waiting for the pH of the soil to rise before germinating. Sugar beet can only be grown in neutral or alkaline soils, and so farmers cannot utilise this sensitivity of the fungus to avoid infection.

Polymyxa betae has been found in soil almost everywhere sugar beet is grown, even where there are no reported cases of rhizomania. The fungus does not always contain the infective virus. In a study in the Netherlands, as little as $10-15\%$ of resting spores contained the virus [17]. Since the cysts can remain dormant for many years, crop rotation will not halt rhizomania infection in a particular field. However, if the initial level of fungus in a particular field is low, it may take one or two successive crops of sugar beet on that field to build up a high level of infection.

The spread of rhizomania has mainly been due to the exchange of seeds and seedlings between distant farms, possibly carrying small amounts of infected soil. The virus has not been successfully transmitted via seed, and so it is likely that soil carries the infection. The ease with which this is accomplished has been demonstrated [1]. Therefore the spread of infection can be contained by measures such as cleaning seed before planting. The other main method of spread of infection is transportation of cystori in the water supply to neighbouring farms, by various methods. The wa-

ter table may be contaminated by drainage, irrigation of sugar beet, or cleaning of harvested sugar beets.

We can summarise the mechanics of the plant-fungi interaction as shown in Figure 1.5. The primary zoospores are released by the fungal cysts in the soil and swim through the soil, apparently attracted by the sugar beet plants. The zoospores then attach themselves to a section of fibrous root, before going into a period of encystment, during which time the stachel is formed and pierces the cell wall, allowing the virus and fungus to enter the plant, see Figure 1.4. Once the fungus is inside the cell, it

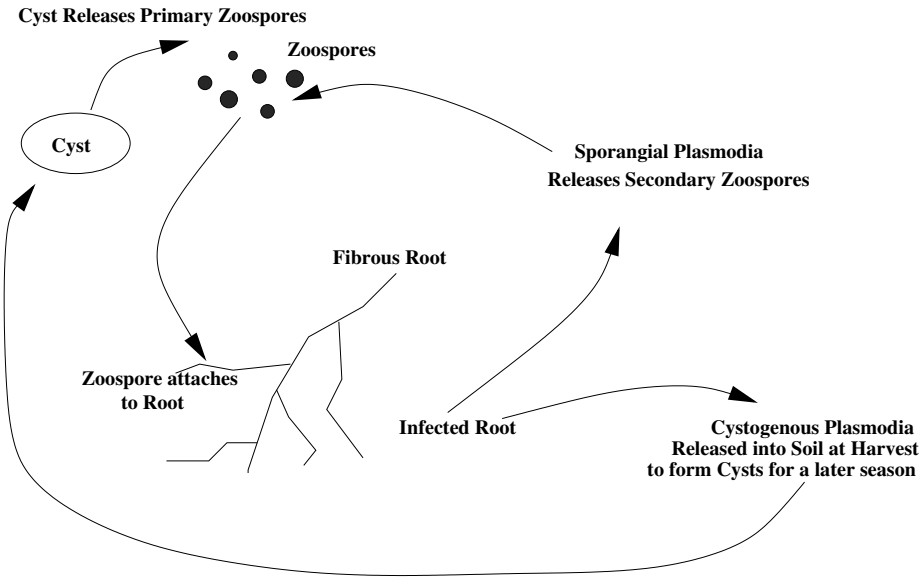

Figure 1.5: Diagrammatic representation of the interaction of the the sugar beet plant with the *Polymyxa betae* fungus.

forms into either a sporangial or cystogenous plasmodia. The sporangial plasmodia releases secondary zoospores into the soil, which then infect further sections of root. The cystogenous plasmodia form cysts which are released into the soil at harvest, and can remain dormant in the soil for many years. If these cysts germinate, the cycle of infection begins again.

1.2 Aims of Modelling

The purpose of this dissertation is to attempt to understand the interaction of the fungus and the plant through a suitable mathematical model. The initial version of this model is outlined in Chapter 2, as described in Truscott *et al* [16] and Webb *et al*, [20]. The specific issues which may be addressed using a mathematical model are the understanding of the spread of the disease, the persistence of infection and the evolution of an infection through a growing season. We shall also address the sensitivity of this model to varying particular parameters.

The model we shall consider is a compartmental model, which assumes that the zoospores and roots are 'well-mixed', i.e. that there is a sufficiently large quantity of both. This compartmental model is based on the primary and secondary infection epidemiological models outlined in Gilligan and Kleczkowski [7]. Of particular interest to biologists is the efficacy of the primary, as opposed to the secondary infection cycle. The primary infection is driven by the primary spores and is limited by the number of such spores supplied to the system. The secondary infection is driven by the secondary spores, and could lead to large infections due to this system feeding back on itself. The biologists would like to know conditions under which each infection dominates, since if the secondary infection dominates, the infection is likely to be worse the following year. Also of interest are two extensions to the model which are the effect of temperature variation and the use of heterogeneous mixing terms. These are discussed in Chapter 4, along with a constant growth term for susceptible roots.

Chapter 2

Modelling Rhizomania

In this chapter we describe the compartmental epidemiological models of Truscott *et al* [16] and Webb *et al* [20]. These models are based on the assumption that the interacting parts are 'well-mixed'. This is a reasonable assumption since the beets are planted relatively close together, as shown in Figure 2.1. Thus, the zoospores do not have far to travel between susceptible fibrous roots. The biological processes involved in rhizomania have been discussed in Chapter 1. In modelling this disease, we only consider the interaction between the fungal vector, *Polymyxa betae*, and the fibrous roots which are host to the fungi. The subsequent action of the beet necrotic yellow vein virus on the plant is not considered, since we assume that it does not affect the interaction between the plant and fungus. From this point forward 'root' is taken to mean fibrous root. The model is designed to aid the understanding of the interaction between the fungus and the root over a season, thus facilitating a map between the infection in one season and the next.

2.1 The Model

In this section we describe the model of Truscott *et al* [16]. We also consider the differences between this and the model outlined in Webb *et al* [20]. The dynamics of the model are shown in Figure 2.2. The healthy root, N, can become susceptible to infection, becoming part of the susceptible population, S. When this susceptible root interacts with the primary zoospores, P , or the secondary zoospores, Z it either becomes infected, I_P or infectious, I_Z. The infected root, I_P, contains cystogenous plasmodia, which will become resting spores at the end of the season. These sections of root cannot be reinfected, since the whole cell space is taken up with the plasmodia. The infectious root, I_Z, contains sporangial plasmodia, which will produce secondary zoospores, Z. Once the secondary zoospores have been released, the root can be reinfected, and so rejoins the susceptible population, S. Susceptible roots become resistant with age, and so join the resistant population R. The root is considered in

Figure 2.1: Three healthy sugar beet plants growing in a field. Reproduced from [15].

units of length per unit volume (cm^{-2}), and the primary and secondary zoospores, P and Z, as spores per unit volume (cm^{-3}).

The interaction between these variables is described in the following system of ordinary differential equations.

$$\text{Total:} \quad \frac{dN}{dt} = rN\left(1-\frac{N}{K}\right) = G(t), \tag{2.1}$$

$$\text{Susceptibles:} \quad \frac{dS}{dt} = G(t) - \lambda_1 SP - \lambda_2 SZ - mS + \sigma I_Z, \tag{2.2}$$

$$\text{Exposed:} \quad \frac{dE}{dt} = \lambda_1 SP + \lambda_2 SZ - \beta_1 E - \beta_2 E, \tag{2.3}$$

$$\text{Infectious:} \quad \frac{dI_Z}{dt} = \beta_1 E - \sigma I_Z, \tag{2.4}$$

$$\text{Infected:} \quad \frac{dI_P}{dt} = \beta_2 E, \tag{2.5}$$

$$\text{Resistant:} \quad \frac{dR}{dt} = mS, \tag{2.6}$$

$$\text{Secondary Zoospores:} \quad \frac{dZ}{dt} = \gamma I_Z - \eta SZ - \alpha Z, \tag{2.7}$$

$$\text{Primary Zoospores:} \quad \frac{dP}{dt} = -\epsilon P \tag{2.8}$$

The assumptions on which this model is based are as follows,

- There is logistic growth of the total root, N, which is not affected by the infection. We could more generally take $G(t)$ as a prescribed function of time, as discussed in Section 2.1.1.
- Susceptible root becomes resistant with age, and this is represented by the terms mS, in (2.2) and (2.6). The amount of susceptible root which becomes resistant

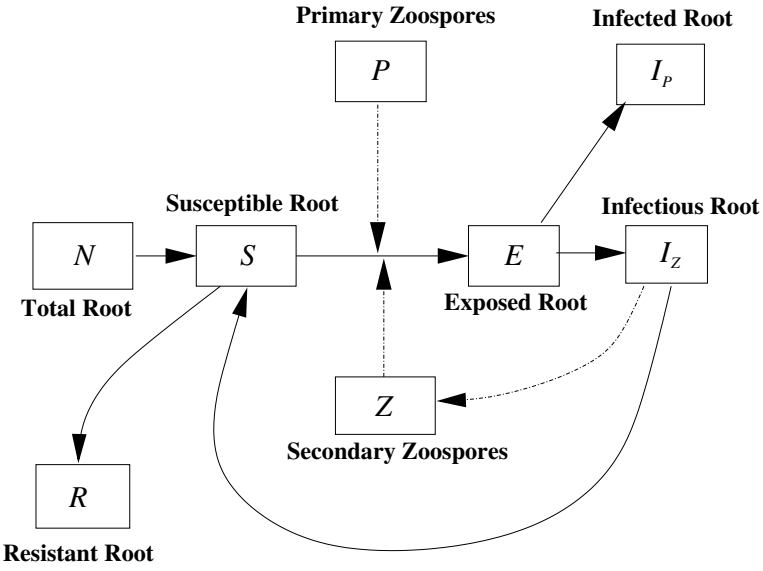

Figure 2.2: Diagrammatic representation of the interaction between the elements of the compartmental model.

is proportional to the existing amount of susceptible host material.

- The infection terms are governed by the law of mass action.
- A section of susceptible root can be exposed to infection by the primary or secondary zoospores. The primary infection is represented by the $\lambda_1 SP$ terms, removing the susceptible root from the susceptible population S and adding it to the exposed population, E.
- The secondary infection removes susceptible root to the exposed root at a rate $\lambda_2 SZ$. It also depletes the number of secondary zoospores at a rate ηSZ since this infection is caused by the secondary zoospores, Z.
- There is a latent period between infection and release of zoospores, or formation of sporangial and cystogenous plasmodia, represented by the $\beta_1 E$ and $\beta_2 E$ terms in (2.3), (2.4) and (2.5). The root remains exposed, E, for a time, $\beta_{1,2}^{-1}$, until the plasmodia are formed and the root becomes infectious or infected.
- Infectious material becomes susceptible at a rate σ, once it has released the secondary zoospores.
- The infectious roots produce secondary zoospores at a rate proportional to the amount of infectious material, represented by the γI_Z term in (2.7).
- Secondary zoospores decay at a rate α, in the absence of infection.

- Infected roots contain cystogenous plasmodia. These sections of root will go on to produce resting spores for the next season.
- The primary zoospores die in the absence of infection of host material, at a rate proportional to the amount of primary zoospores. This exponential decay is represented by the $-\epsilon P$ term in (2.8).
- The variables have no spatial dependence
- There is no variation in temperature, soil moisture or soil texture.

The conservation law for this system of equations is

$$N = S + E + I_Z + I_P + R. \tag{2.9}$$

The initial conditions are that there is a small quantity of fibrous root, which is susceptible, $N(0)$, and primary zoospores, $P(0)$, while everything else is initially absent, since there is no infection.

There are some differences between this model and that of Webb *et al* [20]. Webb *et al*, assume that infectious material cannot be reinfected, whereas in Truscott *et al* it returns to the susceptible population at a rate σ.

2.1.1 Growth of Susceptible Fibrous Root

There are many possible growth functions, $G(t)$. The logistic growth of the total root system, as used in Truscott *et al* [16], is

$$\frac{dN}{dt} = rN\left(1 - \frac{N}{K}\right), \tag{2.10}$$

which can be solved to give

$$N(t) = \frac{N(0)K}{N(0) + (K - N(0))\exp(-rt)}. \tag{2.11}$$

This describes a curve such as that shown in Figure 2.3(a). This form of the growth curve is typical of many biological systems. The growth rate is initially slow, increases in the middle section, before slowing again as the maximum root density, K, is approached.

A similar form of growth is 'monomolecular'

$$N(t) = K - (K - N(0))\exp(-rt). \tag{2.12}$$

This is shown in Figure 2.3(b), with the growth tending exponentially to the maximum density. This form is used by Truscott *et al* in the approximation of quantities in the analysis of the model.

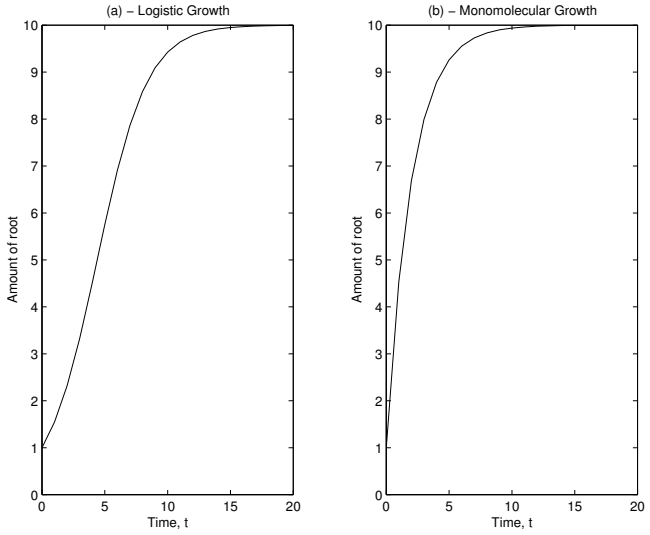

Figure 2.3: Examples of different growth terms, (a) logistic, (b) monomolecular, as in equations 2.11 and 2.12 respectively. In these examples, $K = 10$ cm^{-2}, $N(0) = 1$ cm^{-2}, $r = 0.5$ days^{-1}.

As described in Chapter 1, the infection of the fibrous roots of the sugar beet plant by *Polymyxa betae* mainly occurs at the tips of the fibrous roots. Since the plant is continually expanding its fibrous root system throughout the season [5] this suggests that a constant $G(t)$ would be more suitable.

In our analysis of the model, we consider using each of these forms for the growth function.

2.2 Parameter Values

The parameters in this model are dependent on the quantities represented by S, E, Z etc. In Truscott *et al* [16], the root terms, N, S, E, I_Z, I_P and R are measured as root length per unit volume, with units cm^{-2}. The spore terms, Z and P, are measured in the number of spores per unit volume, with units cm^{-3}. The parameter values used in Truscott *et al* are derived from those in Webb *et al* [20]. This is a slightly different model, as discussed in Section 2.3. The parameter values are selected using experimental data, when such data is available. If there is no suitable data, Webb *et al* have chosen a 'sensible value'. The parameters used in Truscott *et al* and Webb *et al* are shown in Table 2.1 and discussed below.

Growth rate of fibrous roots, r

The growth of the fibrous root system of a sugar beet plant occurs at varying rates throughout a season [5]. The rate of growth, r, in Truscott *et al* is 0.09 days^{-1}. When

this parameter (with K, below) is used in a logistic model of growth for N, the results suggests that the plant has reached its maximum root density after only a small part of the season. This may be inconsistent with field observations [3].

Maximum fibrous root density, K

Sugar beets develop a maximum fibrous root of up to $50,000$ cm after 100-150 days [20]. The average area of land occupied by a sugar beet plant is approximately 750-1000 cm^2 (15-20 cm by 50 cm) [20], to a depth of approximately 120 cm. This suggests that the maximum carrying capacity, K, is 0.56 cm^{-2}. However, in [16], the maximum carrying capacity is given as 10 cm^{-2}, which is rather large.

Average period of root susceptibility, m^{-1}

The time period over which the newly formed root is susceptible, m^{-1}, is not known, but is believed to be a short period, as discussed in Chapter 1. It is chosen to be 10 days in Truscott *et al.*

Rate of infection per unit concentration of zoospores, $\lambda_{1,2}$

The transmission and decay parameters are based on experimental data in [18] and [19]. The most probable number technique is used in these papers to estimate the number of spores in the soil. Approximately 50 resting zoospores are required for one infection. If ten infections occur per day for unit concentration of zoospores, then $\lambda_{1,2} = 0.002$ cm^3 day^{-1} is the rate of infection.

Rate of loss of secondary zoospores due to infection, η

The rate at which secondary spores, Z are lost to infection, η, which should be related to λ_1, is chosen to be 0.05 $\text{cm}^2\text{day}^{-1}$.

Average latent period prior to generation of primary and secondary zoospores, $\beta_{1,2}^{-1}$

The period over which the zoospores develop into sporangial or cystogenous plasmodia is highly dependent on temperature. Since this model does not allow for temperature variation, the results from experiments at $25/circ$C (the optimum temperature for proliferation of the disease) were taken. The average latent periods were $\beta_1^{-1} = 2$ days, for cystogenous plasmodia and $\beta_2^{-1} = 5$ days for sporangial plasmodia.

Rate of release of secondary zoospores, γ

The number of zoospores produced by a sporangial plasmodia in an infectious root can lie in the range $50 - 200$. In Truscott *et al*, γ is taken to be 80 zoospores per unit

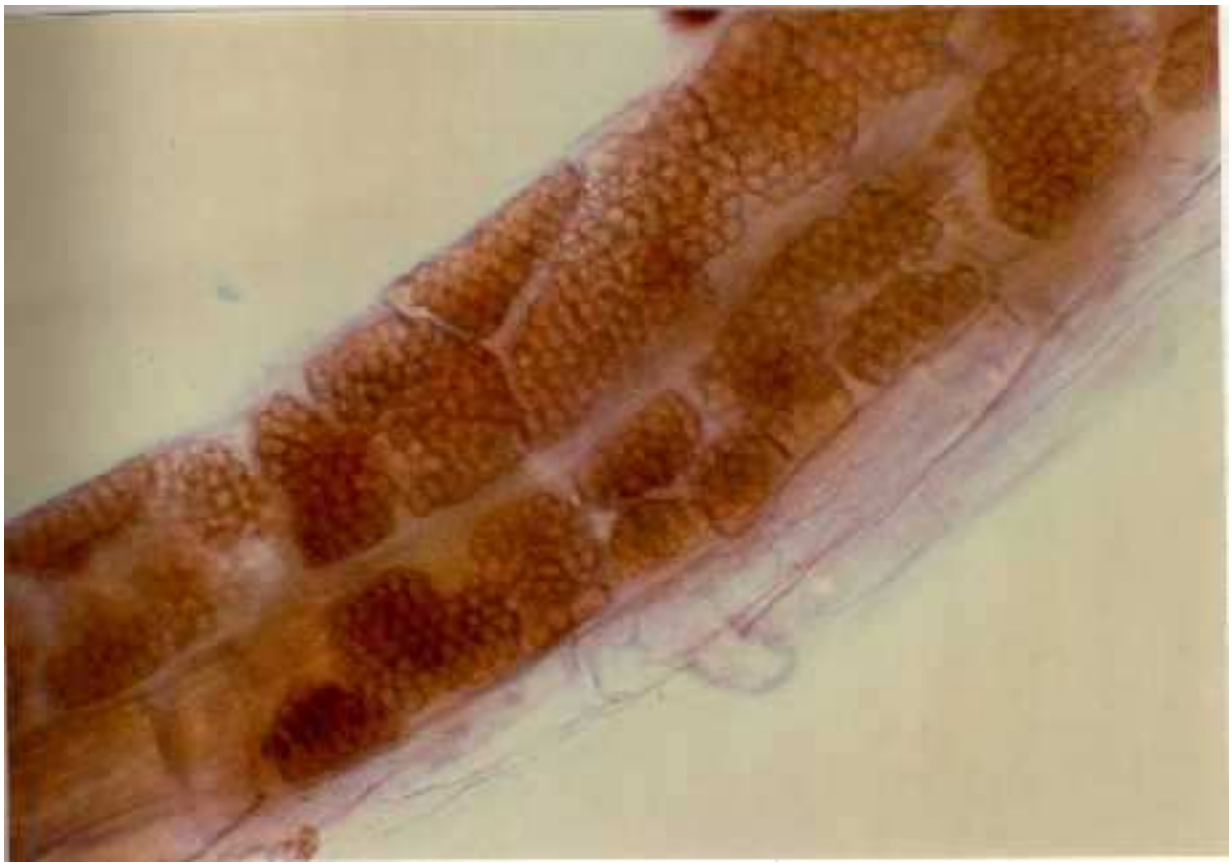

Figure 2.4: Picture of fibrous root cells of a sugar beet seedling containing plasmodia of various shapes and sizes (×470). Reproduced from [3].

length of infected root per day.

Rate of decay of secondary zoospores, α^{-1}

The zoospores can survive only about a day or so in the soil, in the absence of infection, and so $\alpha^{-1} = 1.25$ days.

Length of Root Infected by a Single Zoospore

In both models the parameters λ_2 and η are assumed to be independent. However, consideration of the model shows that this cannot be the case. The ratio λ_2/η represents the length of root that a single spore infects. In Truscott *et al* this ratio is 0.02 cm. In Figure 2.4 we can see that the length infected by a single spore is approximately 0.001-0.006 cm (approximately 0.5-2.5 cm on the figure). This would suggest that η is a factor of 10 too small, or that λ_2 is too large.

	Definition	Truscott *et al* [16]		Webb *et al* [20]	
		Units	Value	Units	Value
r	Growth rate of fibrous roots	days^{-1}	0.09	cm day^{-1}	0.14
K	Maximum fibrous root density	cm^{-2}	10	cm U_a^{-1}	50,000
λ_1	Rate of infection per primary zoospore	$\text{cm}^3\ \text{day}^{-1}$	0.002	$\text{U}_a\ \text{day}^{-1}$ zoospores^{-1} †	0.02
λ_2	Rate of infection per secondary zoospore	$\text{cm}^3\ \text{day}^{-1}$	0.002	$\text{U}_a\ \text{day}^{-1}$ zoospores^{-1} †	0.002
m^{-1}	Average period of root susceptibility	days	9	days	20
β_1^{-1}	Average latent period prior to release of secondary zoospores	days	2	days	2.5
β_2^{-1}	Average latent period prior to generation of resting spores	days	5	days	10
σ^{-1}	Average period over which roots are infectious	days	1	days	1.25
γ	Rate of release of secondary zoospores	$\text{day}^{-1}\ \text{cm}^{-1}$	50	$\text{cm}^{-1}\ \text{day}^{-1}$ zoospores	80
α^{-1}	Average survival time of secondary zoospores	days	2	days	1.25
η	Rate of loss of secondary zoospores through infection	$\text{cm}^2\ \text{days}^{-1}$	0.05	$\text{U}_a\ \text{cm}^{-1}\ \text{days}^{-1}$	0.1
ϵ	Rate of decay of primary zoospores	day^{-1}	0.01	$\text{U}_a\ \text{cm}^{-1}\ \text{days}^{-1}$ *	0.1

Table 2.1: Parameter definitions, units and values as used in Truscott *et al* [16] and Webb *et al* [20]. † There are no 'zoospores' in these units in Webb *et al*. * In this model ϵ is the coefficient shown in 2.16.

2.3 Webb *et al* Model

In Webb *et al* [20] an almost identical model to the one described above is developed. The main difference between the models is that the dependent variables are measured in a different way. The quantity U_a is defined as the area occupied by a single sugar beet plant, approximately 750-1000 cm^2 (15-20 cm by 50 cm). The root terms, N, S, E, I_Z, I_P and R are measured as root length per area occupied by a sugar beet plant, with units cm U_a^{-1}. The spores, Z and P, are measured in the number of spores per area occupied by a single sugar beet plant, with units zoospores U_a^{-1}. The parameter values for this model are shown in Table 2.1.

This model can be interpreted as the original model integrated over the depth of the plant. This means that the linear terms will remain the same, while the nonlinear terms can be approximated by multiplying by a typical length scale, l, say. For example let us consider equation (2.7) and integrate it over a depth, l. We shall use the superscript ^{W} to denote the variables and parameters as they appear in Webb *et al*.

$$\begin{aligned}
\int_0^l \frac{dZ}{dt} dz &= \int_0^l \gamma I_Z - \eta S Z - \alpha Z dz, \\
\Rightarrow \frac{dZ^W}{dt} &= \gamma I_Z^W - \eta \int_0^l S Z dz - \alpha Z^W, \qquad (2.13) \\
\frac{dZ^W}{dt} &\simeq \gamma I_Z^W - \eta l \int_0^l S dz \int_0^l Z dz - \alpha Z^W, \qquad (2.14) \\
\frac{dZ^W}{dt} &\simeq \gamma I_Z^W - \eta^W S^W Z^W - \alpha Z^W. \qquad (2.15)
\end{aligned}$$

Thus, the coefficients of the nonlinear terms in the two models should be approximately related by this length scale, while the coefficients of the linear terms should be the same. Table 2.1 shows that the linear coefficients are of similar size, but there appears to be no consistent relationship between the coefficients of the nonlinear terms.

The main difference in the modelling assumptions between the Webb *et al* and Truscott *et al* models is that Webb *et al* assume that the removal of primary zoospores ($-\epsilon P$ in Truscott *et al*) is due to the infection of susceptible root, and therefore (2.8) becomes

$$\frac{dP}{dt} = -\epsilon S P, \qquad (2.16)$$

The parameters ϵ and λ_2 must be related in this case.

2.4 Discussion

In this chapter we have outlined the model presented in Truscott *et al*, and suggested alternative functional forms and parameter values. In the next chapter we shall

initially use the parameter values from Truscott *et al* in our analysis of the model, for consistency. Later we shall explore the effect of varying these parameters. As discussed in Chapter 1, of particular interest in this system are the roles of the primary and secondary infections. The primary infection is driven by the primary zoospores, and is limited by the number of such zoospores supplied to the system. The secondary infection is driven by the production of secondary zoospores, which can allow feedback, leading to much more infection. In our analysis of the equations in Chapter 3, we aim to give some insight into these different cycles, and the conditions under which each dominates. A possible measure for the relative dominance of the secondary infection to the primary infection would be $\lambda_2 Z_{max}/\lambda_1 P(0)$. In Chapter 4 we shall extend the model to include the effect of temperature variation, introduce heterogeneous mixing terms and discuss the form of the growth term.

In Chapters 3 and 4, the system of ordinary differential equations are solved numerically using Matlab 5 [8]. The system was stiff for some parameter values, and we required moderate levels of accuracy. For this reason, the solver used is 'ode15s' which is described [8] as

> An implicit, multistep numerical differentiation solver of varying order (1-5). Suitable for stiff problems that require moderate accuracy.

Chapter 3

Analysis of the Model

In this chapter we analyse the model presented in Truscott *et al* [16]. The analysis is designed to identify conditions under which a primary or secondary infection occurs. A primary infection is distinct from a secondary infection because the amount of infectious, exposed and infected material will be much higher. In this chapter we also aim to give insight into the map of the infection from one season to another.

3.1 Nondimensionalisation

In their 1997 paper, Truscott *et al* [16] use the following nondimensionalisation of (2.1) to (2.8). The root terms are scaled with the maximum root capacity, K and time is scaled by m^{-1}, the average period of susceptibility. The nondimensionalisation is

$$N = Kn, \qquad S = Ks, \qquad E = Kx, \qquad I_Z = Kc, \qquad I_P = Kc_p, \tag{3.1}$$

$$R = Ku, \qquad Z = \frac{K\gamma}{m}z, \qquad P = Kp, \qquad t = \frac{\tau}{m}, \tag{3.2}$$

where ψ is the number of cystori produced per unit length of infected root. This parameter can then be used in the calculation of the inoculum, p, produced for the next season. The values $1/\psi$ and λ_2/η must be related. For convenience in this calculation, Truscott defines $p_0 = P(0)/\psi K$. This gives the following equations

$$\text{Total:} \quad \frac{dn}{d\tau} = \rho n\,(1-n) = g(\tau), \tag{3.3}$$

$$\text{Susceptibles:} \quad \frac{ds}{d\tau} = g(\tau) - \epsilon_1 sp - \epsilon_2 sz - s + \kappa c, \tag{3.4}$$

$$\text{Exposed:} \quad \frac{dx}{d\tau} = \epsilon_1 sp + \epsilon_2 sz - b_3 x, \tag{3.5}$$

$$\text{Infectious:} \quad \frac{dc}{d\tau} = b_1 x - \kappa c, \tag{3.6}$$

$$\text{Infected:} \quad \frac{dc_p}{d\tau} = b_2 x, \tag{3.7}$$

Parameter	Value		Parameter	Value	
	Truscott *et al* [16]	From Values in Table 2.1		Truscott *et al* [16]	From Values in Table 2.1
ρ	0.8182	0.81	ϵ_1	0.1818	0.18*
κ	9.091	9	ϵ_2	78.5	81
b_1	4.55	4.5	θ	21.59	4.5
ξ	4.55	4.5	b_2	1.82	1.8
p_0	0.1	0.1*	ω	0.091	0.09
b_3	6.37	6.3			

Table 3.1: Nondimensional parameter values, as given in Truscott *et al* [16], and calculated from the values given in Table 2.1. * The values of $P(0)$ and ψ are not given in this paper, but must be approximately by $P(0) = 10$, and hence $\psi = 10$.

$$\text{Resistant:} \quad \frac{du}{d\tau} = s, \tag{3.8}$$

$$\text{Secondary Zoospores:} \quad \frac{dz}{d\tau} = c - \theta sz - \xi z, \tag{3.9}$$

$$\text{Primary Zoospores:} \quad \frac{dp}{d\tau} = -\omega p, \tag{3.10}$$

with initial conditions,

$$(n, s, x, c, c_p, u, z, p) = (n_0, n_0, 0, 0, 0, 0, 0, p_0). \tag{3.11}$$

The nondimensional parameters are

$$\rho = \frac{r}{m}, \qquad \epsilon_1 = \frac{\lambda_1 P(0)}{m}, \qquad \epsilon_2 = \frac{\lambda_2 K\gamma}{m^2} \qquad \kappa = \frac{\sigma}{m}, \qquad b_{1,2} = \frac{\beta_{1,2}}{m}, \tag{3.12}$$

$$\theta = \frac{\eta K}{m}, \qquad \xi = \frac{\alpha}{m}, \qquad \omega = \frac{\epsilon}{m}, \qquad b_3 = b_1 + b_2. \tag{3.13}$$

Typical values of the nondimensional parameters, as given in Truscott *et al* and calculated from Table 2.1, are given in Table 3.1. It should be noted that the values in this table are not exactly the same, in fact the values of θ are radically different, 21.59 in Truscott *et al* and 4.5 when calculated from the typical dimensional parameters in Truscott *et al*. This appears to be due to an incorrect definition of θ in Truscott *et al*, $\theta = \eta\gamma/m$, rather than $\eta K/m$, which gives the value 22.5 when calculated using the values in Table 2.1. In so far as we wish to reanalyse the results in this paper, we shall focus on this value of $\theta = 21.59$.

The size of the growth rate, $g(t)$, in its different forms, as discussed in section 2.1.1, is of interest. Logistic growth of the form

$$\begin{aligned} g(\tau) &= \rho n\,(1 - n)\,, \\ &\leq \rho, \end{aligned}$$

since $n \leq 1$. Similarly for the monomolecular form

$$\begin{aligned} g(\tau) &= \rho(1 - n_0) \exp(-\rho\tau), \\ &\leq \rho. \end{aligned}$$

If $G(t) = l$, the dimensional growth rate, a constant, then

$$g(\tau) = \frac{l}{Km} \approx l. \tag{3.14}$$

These bounds will be used to determine the importance of this growth term, g, in the equations.

3.2 Analysis in Truscott *et al*

As discussed in Chapter 1, of particular interest is the distinction between the roles of the primary and secondary infection cycles. Truscott *et al* use asymptotic expansions, based on the assumption that ϵ_1 and $\epsilon_2 \to 0$, to consider the primary and secondary infection phases separately. These cycles are represented diagrammatically in Figure 3.1. Table 3.1 shows that while ϵ_1 is small, $\epsilon_2 \approx 80$.

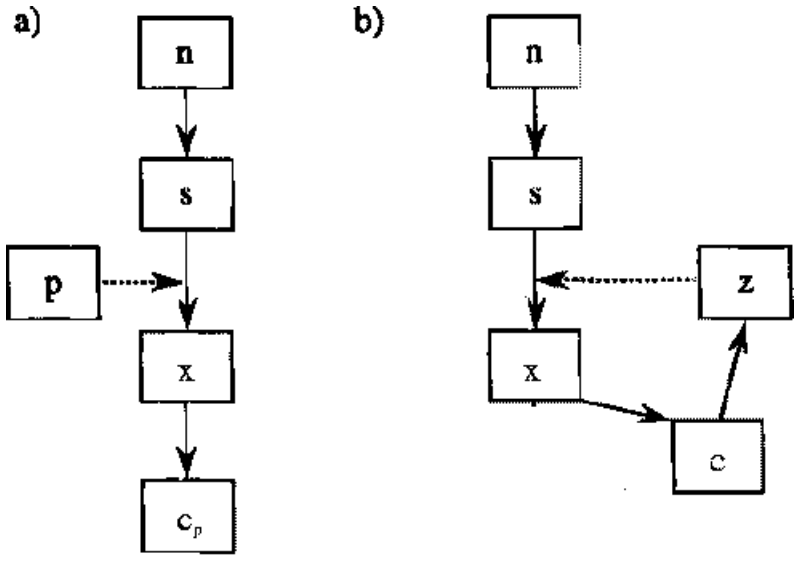

Figure 3.1: The different cycles represented by each order of asymptotics in Truscott *et al*. The first, (a) is the primary cycle, and the second, (b) is the secondary cycle. Adapted from [16].

The asymptotic expansions are of the form

$$s(\tau) = s_0 + \epsilon_1 s_1(\tau) + \epsilon_1\epsilon_2 s_2(\tau) + ... \tag{3.15}$$

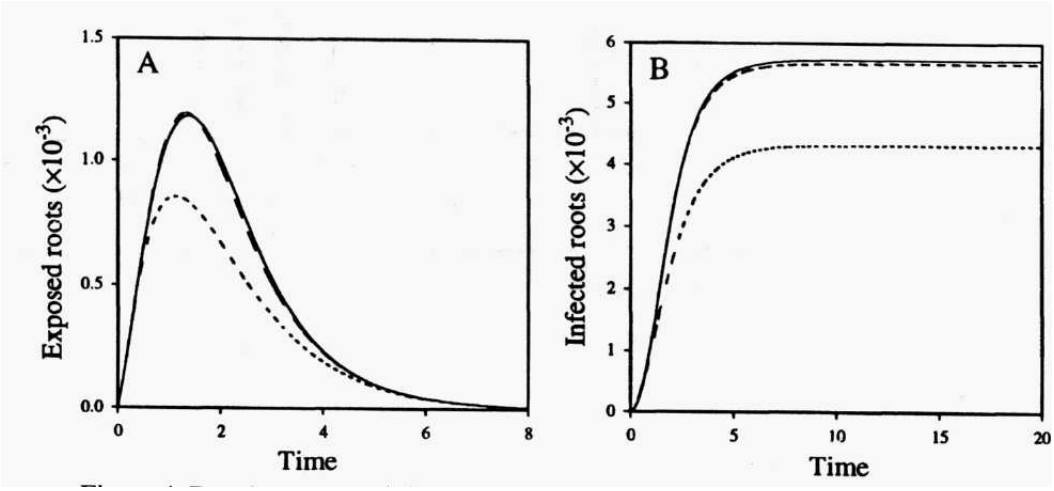

Figure 3.2: Comparison of Truscott's analytical solutions (dotted line first order asymptotic solution, dashed line second order) with numerical solutions (solid line). Reproduced from [16]

The first order solutions to x, the exposed roots, and c_p, the infected roots, using these asymptotic expansions are given in the paper as

$$\begin{aligned} x(\tau) &= \epsilon_1 \left[\left(n_0 + \frac{q\rho}{1-\rho} \right) \left(\frac{1}{b_3 - \omega - 1} (\exp(-(\omega+1)\tau) - \exp(-\tau) \right) \right. \\ &\quad \left. - \frac{q\rho}{\rho - 1} \left(\frac{1}{b_3 - \omega - \rho} \exp(-(\omega+\rho)\tau) - \exp(-b_3\tau) \right) \right], \qquad (3.16) \\ c_p &= \epsilon_1\epsilon_2 \left[b_2 \left\{ \left(n_0 + \frac{q\rho}{1-\rho} \right) \frac{1}{(b_3 - \omega - 1)(1+\omega)} (1 - \exp(-(\omega+1)\tau)) \right. \right. \\ &\quad - \left(n_0 + \frac{q\rho}{1-\rho} \right) \frac{1}{(b_3 - \omega - 1)b_3} (1 - \exp(-b_3\tau) \\ &\quad - \frac{q\rho}{(\rho-1)(b_3 - \omega - \rho)(\rho + \omega)} (1 - \exp(-(\rho+\omega)\tau)) \\ &\quad \left. \left. + \frac{q\rho}{(\rho-1)(b_3 - \omega - \rho)b_3} (1 - \exp(-b_3\tau)) \right\} \right]. \qquad (3.17) \end{aligned}$$

These solutions are in the case where n is monomolecular, and $q = 1 - n_0$.

In spite of the fact that ϵ_2 is large, the results presented in the paper show that these approximations, particularly on inclusion of the second order terms, agree closely with the numerical solutions, as shown in Figure 3.2. This is surprising since ϵ_2 is so large. It is possible that this success is limited to a particular parameter range.

These solutions are used in Truscott *et al* to calculate an estimate for c_p, which is then used to derive conditions under which the disease will be greater or less in the following season. This is discussed in Section 3.6.

3.3 Rescaling and Initial Analysis

We now present an alternative method of analysis of the system. We note that equations (3.7) and (3.8) decouple from this system of equations. Also, since ω is small in equation (3.10), p is a slowly decaying exponential, $p = p_0 \exp(-\omega\tau)$.

We now consider the remaining equations, with $\theta = 21.59$[1]. Since θ is large, this suggests that z goes quickly to an equilibrium value of $c/\theta s$. If this is the case then $\epsilon_2 sz$ is $O(\epsilon_2 c/\theta)$. The equations for x and c could now be considered as linear equations, forced by the $\epsilon_1 sp$ term. This suggests a rescaling of x and c (and hence c_p) with $\epsilon_1 p_0$, and therefore we rescale z with $\epsilon_1 p_0/\theta$. The rescaling is

$$x, c \text{ (and } c_p) \sim \epsilon_1 p_0, \qquad p \sim p_0, \qquad z \sim \frac{\epsilon_1 p_0}{\theta} \tag{3.18}$$

and the rescaled equations are (using the same notation for the variables)

$$\text{Susceptibles:} \quad \frac{ds}{d\tau} = g + \epsilon_1 p_0 \left(-sp - \frac{\epsilon_2}{\theta} sz + \kappa c\right) - s, \tag{3.19}$$

$$\text{Exposed:} \quad \frac{dx}{d\tau} = sp + \frac{\epsilon_2}{\theta} sz - b_3 x, \tag{3.20}$$

$$\text{Infectious:} \quad \frac{dc}{d\tau} = b_1 x - \kappa c, \tag{3.21}$$

$$\text{Secondary Zoospores:} \quad \frac{1}{\theta}\frac{dz}{d\tau} = c - sz - \frac{\xi}{\theta} z. \tag{3.22}$$

In keeping with the motivating assumption, the rescaled equation for secondary zoospores, (3.22), suggests that z goes quickly to equilibrium in comparison to the other quantities, and so can be considered to be at an equilibrium value, $z = c/s$; the term $\xi z/\theta$ is neglected because ξ/θ is small. The equilibrium value $z = s/c$ is then substituted into equation (3.20). The parameters ϵ_1 and p_0 are typically small, and thus the terms which are multiplied by $\epsilon_1 p_0$ in (3.19) are neglected. The equations which remain are

$$\text{Susceptibles:} \quad \frac{ds}{d\tau} = g - s, \tag{3.23}$$

$$\text{Exposed:} \quad \frac{dx}{d\tau} = sp + \frac{\epsilon_2}{\theta} c - b_3 x, \tag{3.24}$$

$$\text{Infectious:} \quad \frac{dc}{d\tau} = b_1 x - \kappa c, \tag{3.25}$$

The equation for s can be solved, given the growth function g, with solution

$$s = n_0 \exp(-\tau) + \exp(-\tau) \int_0^\tau \exp(r) g(r) dr. \tag{3.26}$$

[1] Bear in mind that this value of θ is incorrect

Equations (3.24) and (3.25) can be written as a linear system of ordinary differential equations, as follows

$$\frac{d}{d\tau}\begin{pmatrix} x \\ c \end{pmatrix} = \begin{pmatrix} -b_3 & \frac{\epsilon_2}{\theta} \\ b_1 & -\kappa \end{pmatrix}\begin{pmatrix} x \\ c \end{pmatrix} + \begin{pmatrix} sp \\ 0 \end{pmatrix}, \tag{3.27}$$

which we shall write as

$$\frac{d}{d\tau}\mathbf{x} = A\mathbf{x} + \mathbf{f}. \tag{3.28}$$

In order to solve this equation, we find the eigenvalues and eigenvectors of the matrix A. The eigenvalues are

$$-\mu_\pm = -\frac{1}{2}(\kappa + b_3) \pm \frac{1}{2}\sqrt{(\kappa - b_3)^2 + 4\epsilon_2 b_1/\theta}. \tag{3.29}$$

The discriminant is positive for all positive ϵ_2, b_1 and θ, and hence the eigenvalues are real, since all our parameters are positive. The eigenvalue $-\mu_-$ is always negative, (μ_- is positive). The second eigenvalue, $-\mu_+$ is negative (μ_+ is positive) provided

$$\kappa b_3 > \frac{\epsilon_2 b_1}{\theta}, \tag{3.30}$$

or equivalently

$$\sigma(\beta_1 + \beta_2) > \frac{\lambda_2 \gamma \beta_1}{\eta}, \tag{3.31}$$

in terms of the original parameters. This is true for the typical parameter values given in Table 2.1, where $\kappa b_3 \approx 54$ and $\epsilon_2 b_1/\theta \approx 16$. It does not hold for the correct value of θ.

The eigenvectors corresponding to these eigenvalues are

$$\mathbf{v}_\pm = \begin{pmatrix} v_\pm \\ 1 \end{pmatrix}, \qquad \text{where} \quad v_\pm = \frac{1}{b_1}(\kappa - \mu_\pm). \tag{3.32}$$

We can construct the matrix of eigenvalues, D, and the corresponding matrix of eigenvectors, P, which are such that $AP = PD$, giving

$$\frac{d}{d\tau}\mathbf{x} = PDP^{-1}\mathbf{x} + \mathbf{f}. \tag{3.33}$$

Thus, if we define $\mathbf{x} = P\mathbf{y}$, we have

$$\frac{d}{d\tau}\mathbf{y} = D\mathbf{y} + P^{-1}\mathbf{f}. \tag{3.34}$$

The pair of equations which this represents can be solved separately, since they decouple, being of the form

$$\begin{pmatrix} \dot{y}_1 \\ y_2 \end{pmatrix} = \begin{pmatrix} -\mu_+ & 0 \\ 0 & -\mu_- \end{pmatrix}\begin{pmatrix} y_1 \\ y_2 \end{pmatrix} + \begin{pmatrix} sp \\ -sp \end{pmatrix}, \tag{3.35}$$

with solutions $y_1 = I_+$ and $y_2 = -I_-$ where

$$I_\pm = \exp(-\mu_\pm \tau)\frac{1}{|P|}\int_0^\tau s(r)p(r)\exp(\mu_\pm r)dr. \tag{3.36}$$

When $\mathbf{y}$ is substituted into $\mathbf{x} = P\mathbf{y}$, the solutions are

$$\begin{aligned} x &= v_+ I_+ - v_- I_-, & (3.37)\\ c &= I_+ - I_-, & (3.38) \end{aligned}$$

where

$$I_\pm = \exp(-\mu_\pm \tau)\frac{1}{|P|}\int_0^\tau s(r)p(r)\exp(\mu_\pm r)dr. \tag{3.39}$$

In order to compare our analytical solution with the first order asymptotic expansions given in Truscott *et al*, we consider monomolecular growth of n, of the form $n = 1 - q\exp(-\rho\tau)$, then (from (3.26)) s is

$$\begin{aligned} s(\tau) &= \left(s(0) - \frac{q\rho}{1-\rho}\right)\exp(-\tau) + \frac{q\rho}{1-\rho}\exp(-\rho\tau)\\ &= A_1\exp(-\tau) + A_2\exp(-\rho\tau), \qquad \text{say.} \end{aligned} \tag{3.40}$$

Thus the integral terms, $I_\pm$ (3.39), in x, c and c_p are

$$\begin{aligned} I_\pm &= \exp(-\mu_\pm\tau)\frac{1}{|P|}\int_0^\tau s(r)p(r)\exp(\mu_\pm r)dr\\ &= -\frac{A_1}{|P|(1-\mu_\pm+\omega)}(\exp(-(1+\omega)\tau) - \exp(-\mu_\pm\tau))\\ &\quad -\frac{A_2}{|P|(\rho-\mu_\pm+\omega)}(\exp(-(\rho+\omega)\tau) - \exp(\mu_\pm\tau))\\ &= B_\pm\exp(-\mu_\pm\tau) - B_{1_\pm}\exp(-(1+\omega)\tau) - B_{\rho_\pm}\exp(-(\rho+\omega)\tau). \end{aligned} \tag{3.41}$$

Substituting this into the expression (3.37) for x gives

$$\begin{aligned} x(\tau) &= v_+B_+\exp(-\mu_+\tau) - v_-B_-\exp(-\mu_-\tau) - (v_+B_{1_+} - v_-B_{1_-})\exp(-(1+\omega)\tau)\\ &\quad -(v_+B_{\rho_+} - v_-B_{\rho_-})\exp(-(\rho+\omega)\tau). \end{aligned} \tag{3.42}$$

Similarly the expression for infectious roots (from (3.38)) is

$$\begin{aligned} c(\tau) &= B_+\exp(-\mu_+\tau) - B_-\exp(-\mu_-\tau) - (B_{1_+} - B_{1_-})\exp(-(1+\omega)\tau)\\ &\quad -(B_{\rho_+} - B_{\rho_-})\exp(-(\rho+\omega)\tau). \end{aligned} \tag{3.43}$$

Substituting the solution for x into the equation for c_p (rescaled from (3.7)) gives

$$\begin{aligned} c_p(\tau) &= \frac{v_+B_+}{\mu_+}(1-\exp(-\mu_+\tau)) - \frac{v_-B_-}{\mu_-}(1-\exp(-\mu_-\tau))\\ &\quad -\frac{(v_+B_{1_+} - v_-B_{1_-})}{(1+\omega)}(1-\exp(-(1+\omega)\tau))\\ &\quad -\frac{(v_+B_{\rho_+} - v_-B_{\rho_-})}{(\rho+\omega)}(1-\exp(-(\rho+\omega)\tau)). \end{aligned} \tag{3.44}$$

Parameter	Definition	Typical Value
μ_+	$\frac{1}{2}(\kappa+b_3)-\frac{1}{2}\sqrt{(\kappa-b_3)^2+4\epsilon_2 b_1/\theta}$	3.5
μ_-	$\frac{1}{2}(\kappa+b_3)+\frac{1}{2}\sqrt{(\kappa-b_3)^2+4\epsilon_2 b_1/\theta}$	11.8
v_+	$\frac{1}{b_1}(\kappa-\mu_+)$	1.2
v_-	$\frac{1}{b_1}(\kappa-\mu_-)$	-0.6
$\|P\|$	$\|v_+-v_-\|$	1.8
A_1	$s(0)-\frac{q\rho}{1-\rho}$	-94
A_2	$\frac{q\rho}{1-\rho}$	94.05
B_+	$\frac{A_1}{\|P\|(1-\mu_++\omega)}+\frac{A_2}{\|P\|(\rho-\mu_++\omega)}$	0.074
B_-	$\frac{A_1}{\|P\|(1-\mu_-+\omega)}+\frac{A_2}{\|P\|(\rho-\mu_-+\omega)}$	0.0019
B_{1_+}	$\frac{A_1}{\|P\|(1-\mu_++\omega)}$	21.2
B_{1_-}	$\frac{A_1}{\|P\|(1-\mu_-+\omega)}$	4.7
B_{ρ_+}	$\frac{A_2}{\|P\|(\rho-\mu_++\omega)}$	-21.2
B_{ρ_-}	$\frac{A_2}{\|P\|(\rho-\mu_-+\omega)}$	-4.7

Table 3.2: Coefficients of analytical solutions, e.g. equation (3.42).

Typical values for these constants are given in Table 3.2.

In Figure 3.3 we compare these expressions, from the linear system, with Truscott's asymptotic expansions and numerical solutions of the full system of equations. As discussed in Chapter 2, the equations were solved numerically using an ordinary differential equation solver in Matlab 5 (by Mathworks), 'ode15s' [8]. Within the context of our approximation, we would expect an error of order ξ/θ, and the results are quite satisfactory.

The total amount of infected material at the end of the season can be approximated by

$$\begin{aligned}\lim_{\tau\to\infty} c_p(\tau) &= \frac{v_+B_+}{\mu_+}-\frac{v_-B_-}{\mu_-}-\frac{(v_+B_{1_+}-v_-B_{1_-})}{(1+\omega)} \\ &\quad -\frac{(v_+B_{\rho_+}-v_-B_{\rho_-})}{(\rho+\omega)}.\end{aligned} \tag{3.45}$$

This will be used in Section 3.6 in mapping the infection from one season to another.

3.4 Primary and Secondary Cycles

In Section 3.2 we have derived an analytical solution for the primary cycle, which agrees well with the numerical solution in the normal parameter range, and conditions under which the primary infection dominates. We shall now investigate what happens when these conditions are violated.

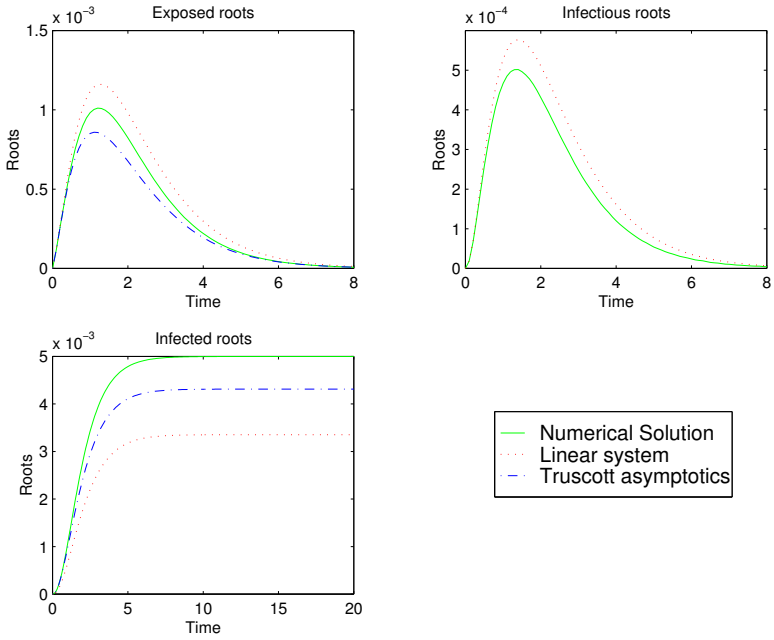

Figure 3.3: Comparing numerical solutions of the system of equations (3.3) to (3.10) (dashed line), (3.19) to (3.22) (dotted line) and (3.23) to (3.25) (solid line), at the parameter values shown in Table 3.1.

If the condition (3.30) is violated, for example if ϵ_2 is large, the zero steady state is no longer stable, and so there must be a bifurcation. In the context of our approximation, the variables will begin growing exponentially. This growth will continue until $z \sim \epsilon_1 p_0 \epsilon_2 s/\theta$, which would make the ξ/θ term important, pulling the solutions back down towards zero. This suggests rescaling in order to make the $\epsilon_1 p_0$ terms important. With this in mind, we perform the following rescaling

$$s \sim \xi/\theta, \qquad c, x \sim \frac{b_3\xi}{\epsilon_1 p_0 \kappa \theta}, \qquad z \sim \frac{b_3}{\epsilon_1 p_0 \kappa \xi}, \qquad t \sim \frac{1}{b_3}. \tag{3.46}$$

This gives the following equations (using the same notation for the dependent variables)

$$\begin{aligned} \nu_1 \dot{z} &= \xi c - (1+s)z, && (3.47)\\ \dot{c} &= \beta x - \nu_2 c, && (3.48)\\ \dot{x} &= \chi s p + \nu_2 \nu_3 s z - x, && (3.49)\\ \dot{s} &= \bar{g} - \nu_3 s z - \frac{1}{b_3} s + c - \frac{\chi}{\nu_2} s p, && (3.50) \end{aligned}$$

where

$$\nu_1 = \frac{b_3}{\xi}, \qquad \nu_2 = \frac{\kappa}{b_3}, \qquad \nu_3 = \frac{\epsilon_2}{\kappa\theta\xi}, \qquad \bar{g} = \frac{\theta}{b_3\xi} g, \qquad \beta = \frac{b_1}{b_3}, \qquad \chi = \frac{\epsilon_1 p_0 \kappa}{b_3^2}. \tag{3.51}$$

Parameter	Value		Parameter	Value	
	Truscott *et al* [16]	From Values in Table 2.1		Truscott *et al* [16]	From Values in Table 2.1
ν_1	1.4	1.4	ν_2	1.427	1.429
ν_3	0.08	0.4	β	0.7143	0.7143
χ	0.004	0.004	$\bar{g}$	$0.7g$	$0.2g$
$1/b_3$	0.16	0.16	ξ	4.5	4.5

Table 3.3: Nondimensional parameter values, as given in Truscott *et al* [16], and calculated from the values given in Table 2.1. Notice that χ and ν_3 are small for the incorrect value of θ, which perhaps explains why Truscott *et al*'s asymptotic expansions are accurate in this region, because ϵ_2 is not important in the rescaled system in this case. If however, the correct value of θ were used, this would no longer be the case.

This is what we shall call the canonical form of the equations. All the coefficients are of order 1 except χ and $1/b_3$ which are small, see Table 3.3. We can see that z and c are small initially. If the growth rate, $\bar{g}$, is small, and c is small, s is slowly varying. Let us assume that this is the case, and s can be considered to be a constant. The remaining system, neglecting the χ term, is

$$\begin{pmatrix} \nu_1 & 0 & 0 \\ 0 & 1 & 0 \\ 0 & 0 & 1 \end{pmatrix} \begin{pmatrix} \dot{z} \\ \dot{c} \\ \dot{x} \end{pmatrix} = \begin{pmatrix} -(1+s) & \xi & 0 \\ 0 & -\nu_2 & \beta \\ \nu_2\nu_3 s & 0 & -1 \end{pmatrix} \begin{pmatrix} z \\ c \\ x \end{pmatrix}. \tag{3.52}$$

We shall write this as

$$A\dot{\psi} = B\psi, \tag{3.53}$$

which has solutions of the form $z, c, x \propto \exp(\lambda t)$, provided $|\lambda A - B| = 0$. The system is stable if the real part of the λ's are negative. The λ's are given by

$$\left| \begin{pmatrix} \nu_1\lambda + (1+s) & -\xi & 0 \\ 0 & \lambda + \nu_2 & -\beta \\ -\nu_2\nu_3 s & 0 & \lambda + 1 \end{pmatrix} \right| = (\nu_1\lambda + (1+s))(\lambda + \nu_2)(\lambda + 1) - \xi\nu_2\nu_3\beta s = 0 \tag{3.54}$$

If $s = 0$, then $\lambda = -\nu_2, -1, -1/\nu_1$ and the system is stable.

Thus, if s is sufficiently small we have a stable system, with the variables remaining small. As s increases, we may have exponential growth, or oscillatory solutions. We shall investigate whether one of these occurs, and whether there is a switch between different types of solution. A switch could happen in one of two ways, through a Hopf bifurcation or through one of the eigenvalues increasing through zero. A Hopf bifurcation occurs when the real part of a pair of complex conjugate roots to this equation increase through zero as some parameter increases, before any real, negative eigenvalues cross through zero.

If we were to assume that there were a Hopf bifurcation, it would be possible to write equation (3.54) as $\nu_1(\lambda^2+\omega^2)(\lambda+c)=0$ where ω^2 and c are real and positive. Let us compare our two forms of this equation,

$$\begin{aligned} 0 &= \nu_1\lambda^3 + c\nu_1\lambda^2 + \nu_1\omega^2\lambda + c\nu_1\omega^2 && (3.55)\\ 0 &= \nu_1\lambda^3 + (1+s+\nu_1+\nu_2\nu_1)\lambda^2 + ((1+s)(1+\nu_2)+\nu_1\nu_2)\lambda \\ &\quad +\nu_2(1+s) - \nu_2\nu_3\beta\xi s. && (3.56)\end{aligned}$$

If these two forms are to match, then

$$\begin{aligned} \text{coefficient of } \lambda^2 \times \text{coefficient of } \lambda &= \nu_1 \times \text{constant term} \\ (1+s+\nu_1+\nu_2\nu_1)((1+s)(1+\nu_2)+\nu_1\nu_2) &= \nu_1(\nu_2(1+s)-\nu_2\nu_3\beta\xi s) \\ \Rightarrow (1+s+\nu_1+\nu_2\nu_1)((1+s)+\nu_1\nu_2)+\nu_1\nu_2\nu_3\beta\xi s &= 0 \qquad (3.57)\end{aligned}$$

This means that a positive quantity (all the parameters are positive, and s is positive) is equal to zero, which is a contradiction. Thus a Hopf bifurcation cannot occur.

Only the real eigenvalue can go through zero and stability is determined by the value of s. If $\lambda=0$, then $s=1/(\nu_3\beta\xi-1)$. Thus, the real eigenvalue is negative (and the system is stable) if $s<1/(\nu_3\beta\xi-1)$; the real eigenvalue is positive (and the system is unstable) if $s>1/(\nu_3\beta\xi-1)$. If

$$\nu_3\beta\xi < 1, \qquad (3.58)$$

the system is always stable, but if $\nu_3\beta\xi>1$, then this represents a threshold value above which secondary infection occurs (as defined earlier). The secondary infection becomes dominant if the maximum value of s is greater than this value.

These three scenarios are demonstrated in the numerical solutions of the equations shown in Figure 3.4, 3.5 and 3.6 . In Figure 3.4, the equations are solved with the Truscott *et al* parameter values, with $\nu_3\beta\xi<1$. The primary infection dominates, with x and c remaining of order $\epsilon_1 p_0$. This is in keeping with our first rescaling. Figure 3.5 shows the case where the threshold $1/(\nu_3\beta\xi-1)$ is positive (=0.5), but s never crosses it. While the x and c variables are higher than in the previous example, they are not significantly so. In Figure 3.6, s is larger than the threshold value (=0.03), and the secondary infection dominates, with x and c becoming much larger than in Figure 3.4. The variable s does not appear to be slowly varying overall. However, in the region where the growth rate, $\bar{g}$, is small, after being initially high, s is slowly varying, and it is here that the other variables either sharply increase or decrease. Figure 3.6 shows this particularly well, with an initial slow growth in x, c and c_p followed by a steep increase. The same behaviour can be seen in Figure 3.5. Figure 3.4, however does not show this, thus agreeing with our analysis, since this is a primary infection.

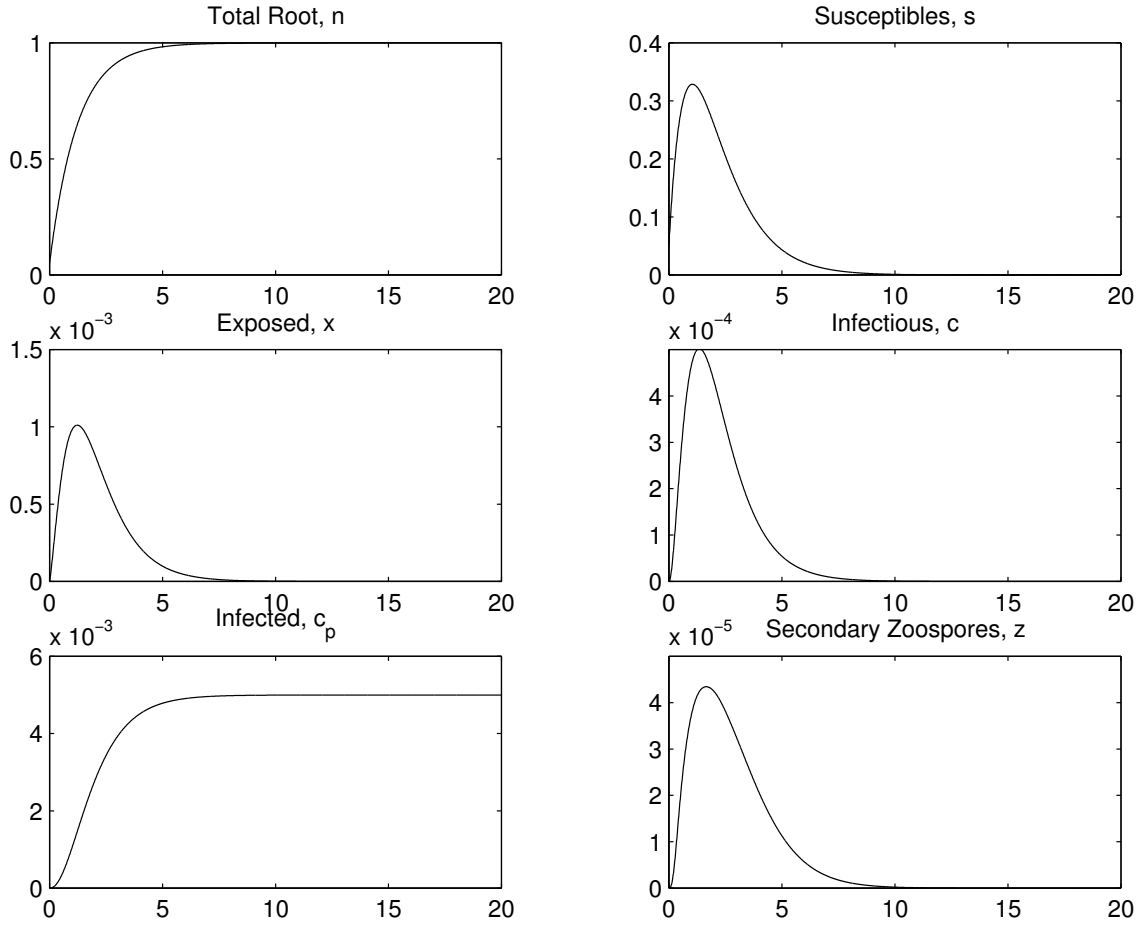

Figure 3.4: Numerical solutions of the system of equations (3.3) to (3.10), against time, τ, with the parameters as in Truscott *et al* (see Table 3.1). The condition $\nu_3\beta\xi < 1$ is satisfied, and the primary infection dominates. The variables x and c are of approximate order $\epsilon_1 p_0$ (≈ 0.03)

Our analysis has led to some insight on the behaviour of these equations, but we shall now formalise the expression 's is slowly varying', using the WKB method. To do this, we consider the equation for s

$$\dot{s} = \bar{g} - \nu_3 sz - \frac{1}{b_3}s + c - \frac{\epsilon_1 p_0}{b_3}sp. \tag{3.59}$$

Now, if $\bar{g}$ and $1/b_3$ are small, and z and c are initially small, then we can define a slow timescale $\tau = \bar{g}t$. The variable s will vary on this timescale, and so $s = s(\tau)$. Now, we return to equation (3.53), and write it as

$$\dot{\psi} = M\psi, \tag{3.60}$$

where $M = A^{-1}B$ (A is nonsingular) and $\dot{} = d/dt$. The WKB method is to write ψ as

$$\psi \sim \exp\left(\frac{\Lambda_0(\tau)}{\bar{g}} + \Lambda_1(\tau) + O(\bar{g})\right)[\mathbf{u}_0(\tau) + \bar{g}\mathbf{u}_1(\tau) + ...] \tag{3.61}$$

Now, our equation is

$$\bar{g}\psi' = M\psi, \tag{3.62}$$

assuming a solution of the form (3.61) where $' = d/d\tau$. This becomes

$$\bar{g}\left\{\frac{1}{\bar{g}}\dot{\Lambda}_0 + \dot{\Lambda}_1 + ...\right\}[\mathbf{u}_0 + \bar{g}\mathbf{u}_1 + ...] + \bar{g}[\dot{\mathbf{u}}_0 + \bar{g}\dot{\mathbf{u}}_1 + ...] = M(\tau)[\mathbf{u}_0 + \bar{g}\mathbf{u}_1 + ...] \tag{3.63}$$

To first order, this gives

$$\dot{\Lambda}_0\mathbf{u}_0 = M\mathbf{u}_0, \tag{3.64}$$

which has nontrivial solutions if $\dot{\Lambda}_0$ is an eigenvalue of M. The leading order solution is

$$\psi \sim \exp\left(\frac{1}{\bar{g}}\Lambda_0(\tau)\right)\mathbf{u}_0(\tau). \tag{3.65}$$

Thus, when we compare this with our linear analysis, obtained by considering s to be constant, with eigenvalues of the linear system, λ, as above, the solutions are

$$\psi \sim \exp\left(\int^t \lambda\, dt\right)\mathbf{u}_0(\tau). \tag{3.66}$$

In principle this could be computed, but the solution would be very complex. The growth and decay of ψ is still determined by the sign of λ, and the transition from primary to secondary infection is still associated with λ passing through zero, since $\dot{\psi}/\psi \sim \lambda$ at a particular instant.

3.5 Corrected Parameters

Correct calculation of θ

If we were to use θ at its correct value of 4.5 (instead of 21.59), as discussed in Section 3.1 the effect would be to increase ν_3 and decrease $\bar{g}$ in equations (3.47) to (3.50). This would not change the main line of analysis, since we have made no assumption about the size of ν_3. If $\bar{g}$ is reduced, then the assumption that $\bar{g}$ is small will be further validated. Thus, the correct calculation of θ would make little difference to the behaviour of the equations. (See Table 3.3 for comment on possible effect of varying θ on Truscott *et al* asymptotic solution)

Length of root infected by a single zoospore, λ_2/η

We now recall Section 2.2, where the ratio of λ_2 to η, the length of root infected by a single zoospores, was considered to be too large in the parameter values presented by Truscott *et al* [16]. If we adjust one or other of the parameters by a factor of 10, the resulting effect on the nondimensional paramters is shown in Table 3.4. This would

Parameter Adjustment	Nondimensional Parameter Affected	Typical Value	
		Before Adjustment	After Adjustment
$\eta \times 10$	θ	4.5	45
	ν_3	0.4	0.04
$\lambda_2/10$	ϵ_2	78	7.8
	ν_3	0.4	0.04

Table 3.4: Nondimensional parameter values, as given in Truscott *et al* [16], and calculated from the values given in Table 2.1.

suggest that when we correct the parameters, $\nu_3 << 1$. If we apply this assumption to equations (3.47) to (3.50), then the equation for x uncouples, and the remaining equations are linear

$$\dot{c} = \beta x - \nu_2 c, \tag{3.67}$$

$$\dot{x} = \chi p s - x, \tag{3.68}$$

$$\dot{s} = \bar{g} - \frac{1}{b_3} s + c - \frac{\epsilon_1 p_0 p}{b_3} s. \tag{3.69}$$

Since $\nu_3 << 1$, then the condition $\nu_3 \beta < 1$ (3.58) holds, suggesting a primary infection cycle. Therefore we would anticipate that the eigenvalues of this system are negative. These eigenvalues, λ, are defined by

$$\left| \begin{pmatrix} -(\nu_2+\lambda) & \beta & 0 \\ 0 & -(\lambda+1) & \chi p \\ 1 & 0 & -\left(\frac{1}{b_3} + \frac{\epsilon_1 p_0 p}{b_3} + \lambda\right) \end{pmatrix} \right| = -(\nu_2+\lambda)(1+\lambda)\left(\frac{1}{b_3} + \frac{\epsilon_1 p_0 p}{b_3} + \lambda\right) + \beta\chi p = 0. \tag{3.70}$$

If $p = 0$ $\lambda = -\nu_2, -1$ (double root), and the system is stable (there is no infection). As in Section 3.4, we consider the possibility of a bifurcation, and consider (3.70) in the form $(\lambda^2 + \omega^2)(\lambda + c) = 0$ where $\omega^2 c > 0$. In this case there cannot be a Hopf bifurcation, by a similar argument to that in Section 3.4. We now note that

$$\frac{\beta\chi}{\nu_2} = \frac{\epsilon_1 p_0 b_1}{b_3^2} < \frac{\epsilon_1 p_0}{b_3}, \tag{3.71}$$

since $b_1 < b_3$. If $\lambda = 0$, then

$$\frac{1}{b_3} + \frac{\epsilon_1 p_0 p}{b_3} = \frac{\beta\chi}{\nu_2} p < \frac{\epsilon_1 p_0}{b_3} p, \tag{3.72}$$

which is a contradiction. Therefore λ cannot be zero and the system is always stable. This means, as expected, that when λ_2 and η are adjusted, the resulting infection is primary.

3.6 Mapping From One Season to the Next

In Truscott *et al* [16] the infection is mapped from one season to the next using the following relation, in terms of the original variables

$$P_{n+1}(0) = P_n(t_f) + \psi I_P(t_f), \tag{3.73}$$

where P_n is the number of primary propagules in season n, which runs from time 0 to t_f, harvest. Since P_n is an exponential, this equation is

$$P_{n+1}(0) = P_n(0)\exp(-\epsilon t_f) + \psi I_P(t_f). \tag{3.74}$$

In terms of the original nondimensionalised variables, this is

$$p_{n+1}(0) = p_n(0)\exp(-\epsilon\tau_f) + c_p(\tau_f). \tag{3.75}$$

In terms of our rescaled variables, in the primary case, this is

$$p_{n+1}(0) = p_n(0)\left(\exp(-\epsilon\tau_f) + \epsilon_1 c_p(\tau_f)\right). \tag{3.76}$$

Since the solution c_p is tending to a constant within the season, we can approximate this by

$$p_{n+1}(0) = p_n(0)\left(\exp(-\omega\tau_f) + \epsilon_1 \lim_{\tau\to\infty} c_p(\tau)\right), \tag{3.77}$$

where $\lim_{\tau\to\infty} c_p(\tau)$ is given in equation (3.45). The change from one season to another can be written

$$\begin{aligned} \Delta p(0) &= p_{n+1}(0) - p_n(0) \\ &= p_n(0)\left(\epsilon_1 \lim_{\tau\to\infty} c_p(\tau) - (\exp(-\omega\tau_f) - 1)\right) \end{aligned} \tag{3.78}$$

Thus the epidemic will 'bulk up' if

$$\epsilon_1 c_p(\infty) > 1 - \exp(-\omega\tau_f) \tag{3.79}$$

and 'fade out' otherwise. Now,

$$c_p(\infty) = b_1 \int_0^\infty x(\tau)\, d\tau \tag{3.80}$$

$$\approx b_1 \times 20 \times \text{ order of } x \tag{3.81}$$

Thus, for a primary infection, the condition for 'bulk up' is approximately

$$20\epsilon_1^2 b_1 p_0 > 1 - \exp(-\omega\tau_f), \tag{3.82}$$

and for a secondary infection

$$\frac{20\epsilon_1 b_1 b_3 \xi}{\kappa\theta} > 1 - \exp(-\omega\tau_f), \tag{3.83}$$

In the secondary infection case, we have not derived an analytical solution, and so can only make genral comments. When $\nu_3\beta\xi > 1$ and s is higher than the threshold value, the amount of c_p increases rapidly, and probably leads to 'bulk up' of the disease.

3.7 Discussion

In this chapter we have derived conditions under which primary and secondary infection will occur, using the condition

$$\kappa b_3 > \frac{\epsilon_2 b_1}{\theta}, \tag{3.84}$$

or

$$\sigma(\beta_1 + \beta_2) > \frac{\lambda_2 \gamma \beta_1}{\eta}, \tag{3.85}$$

in terms of the original parameters for primary infection. This condition is comparing the rate of infection by secondary zoospores λ_2, and the rate of release of secondary zoospores γ with the average survival time of secondary zoospores σ. Thus as the rate of release of secondary zoospores and the rate of infection of these zoospores increase, the primary infection cycle becomes dominated by the secondary infection. The parameters $\beta_{1,2}$, which are a measure of the amount of time taken to form a plasmodium following infection, also play a role in the switch between primary and secondary infection.

The distinction between primary and secondary infection is based on whether certain exponential terms decay or grow. This leads to a smooth transition between to two types of infection as the threshold is passed. The threshold is only indicative of a transition between primary and secondary infections, as shown in Figure 3.7, where there is growth in the maximum value of the variables as $\nu_3 \beta \xi$ passes through the threshold.

In the mapping of the infection from season to season, we have not derived a precise condition for 'bulk up' or 'fade out', but the conditions for primary or secondary infection will have an impact on this, with secondary infection producing much more infectious material for the next season.

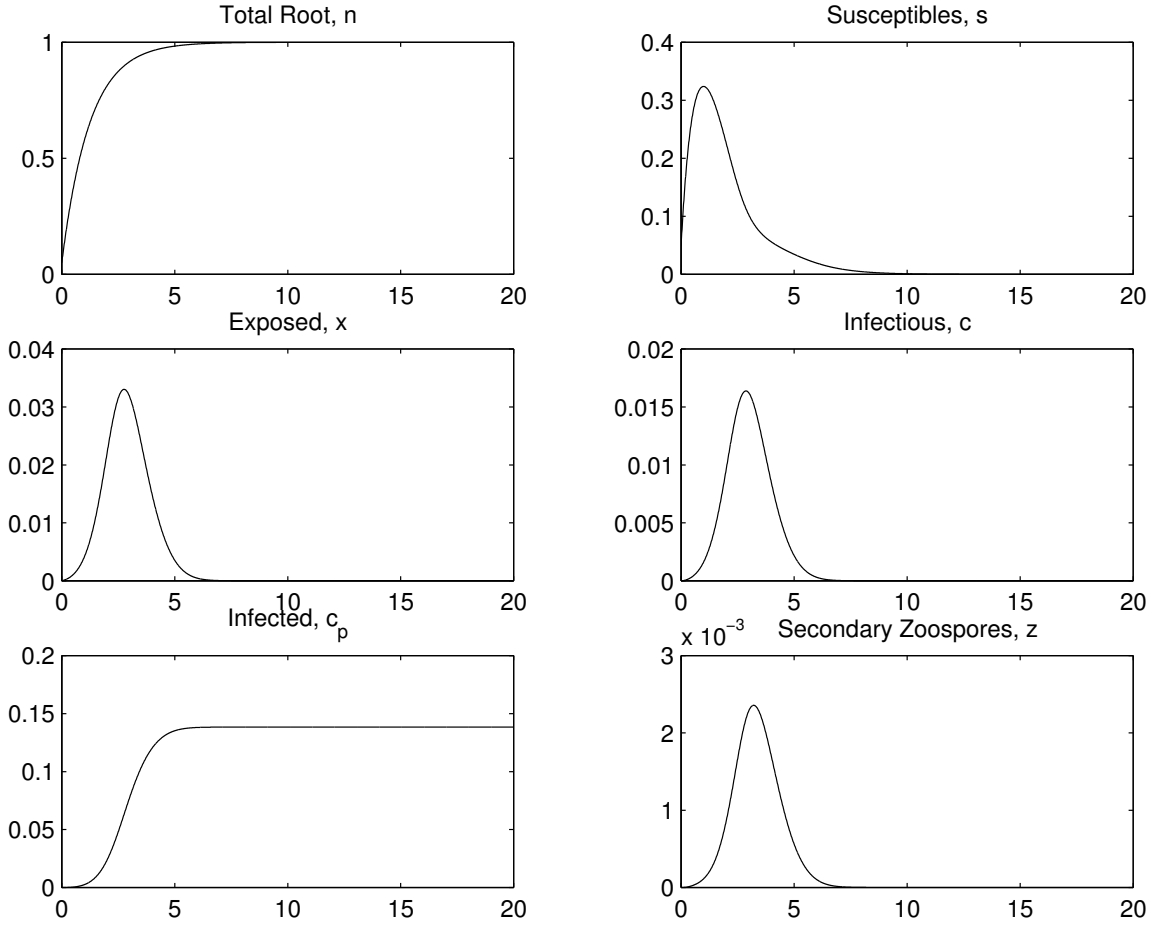

Figure 3.5: Numerical solutions of the system of equations (3.3) to (3.10), against time, τ, with the parameters as in Truscott *et al* (see Table 3.1), except ϵ_2 has been multiplied by a factor of 10. The condition $\nu_3\beta\xi > 1$ is satisfied, and the secondary infection is becoming more prominent than in Figure 3.4, since the exposed, infected and infectious variables are becoming larger. However, $s < 1/(\nu_3\beta\xi - 1) = 0.5$, and so the threshold has not been passed. The variables x and c are of approximate order $b_3\xi/\theta(= O(1))$, as the rescaling supposed.

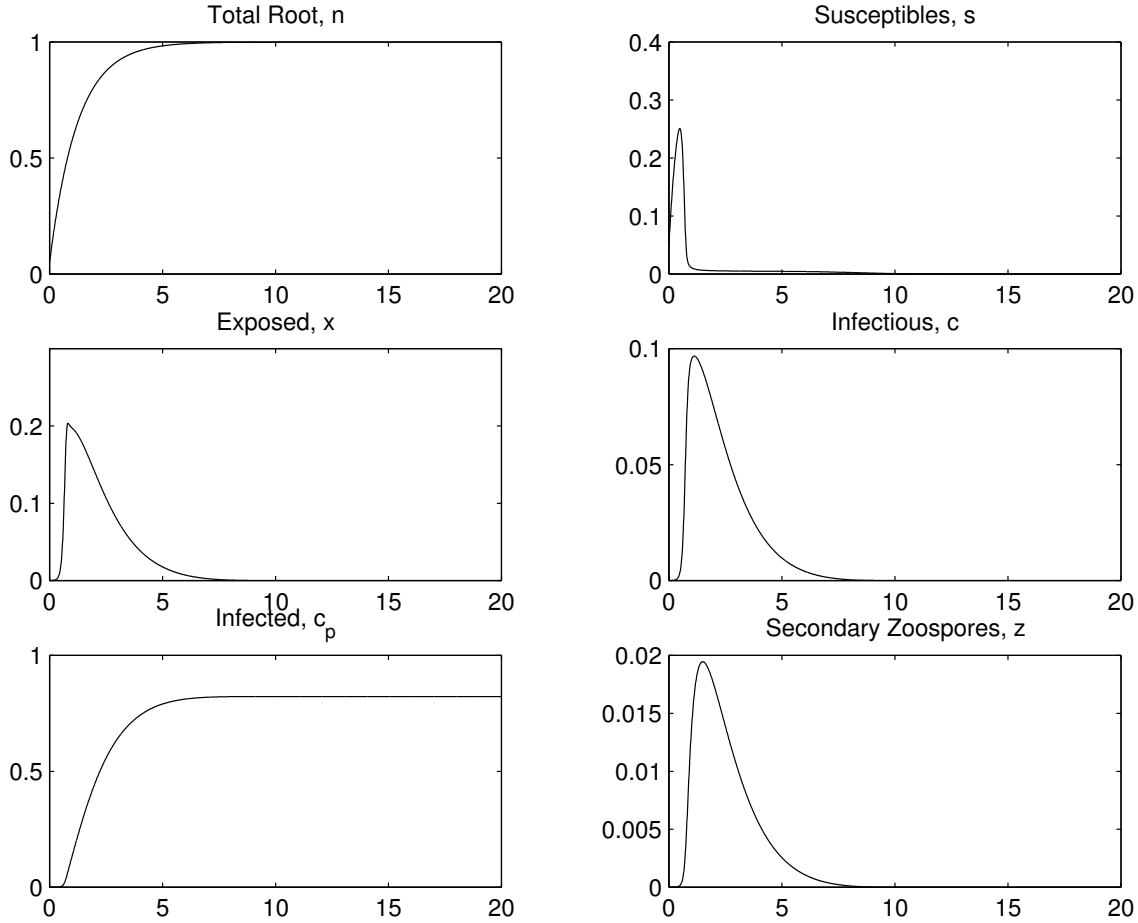

Figure 3.6: Numerical solutions of the system of equations (3.3) to (3.10), against time, τ, with the parameters as in Truscott *et al* (see Table 3.1), except ϵ_2 has been multiplied by a factor of 100. The condition $\nu_3\beta\xi > 1$ is satisfied, and the secondary infection is dominant, since the exposed, infected and infectious variables are much larger. The variable $s > 1/(\nu_3\beta\xi - 1) = 0.03$, and so the threshold condition is satisfied, leading to large exposed, infectious and infected variables.

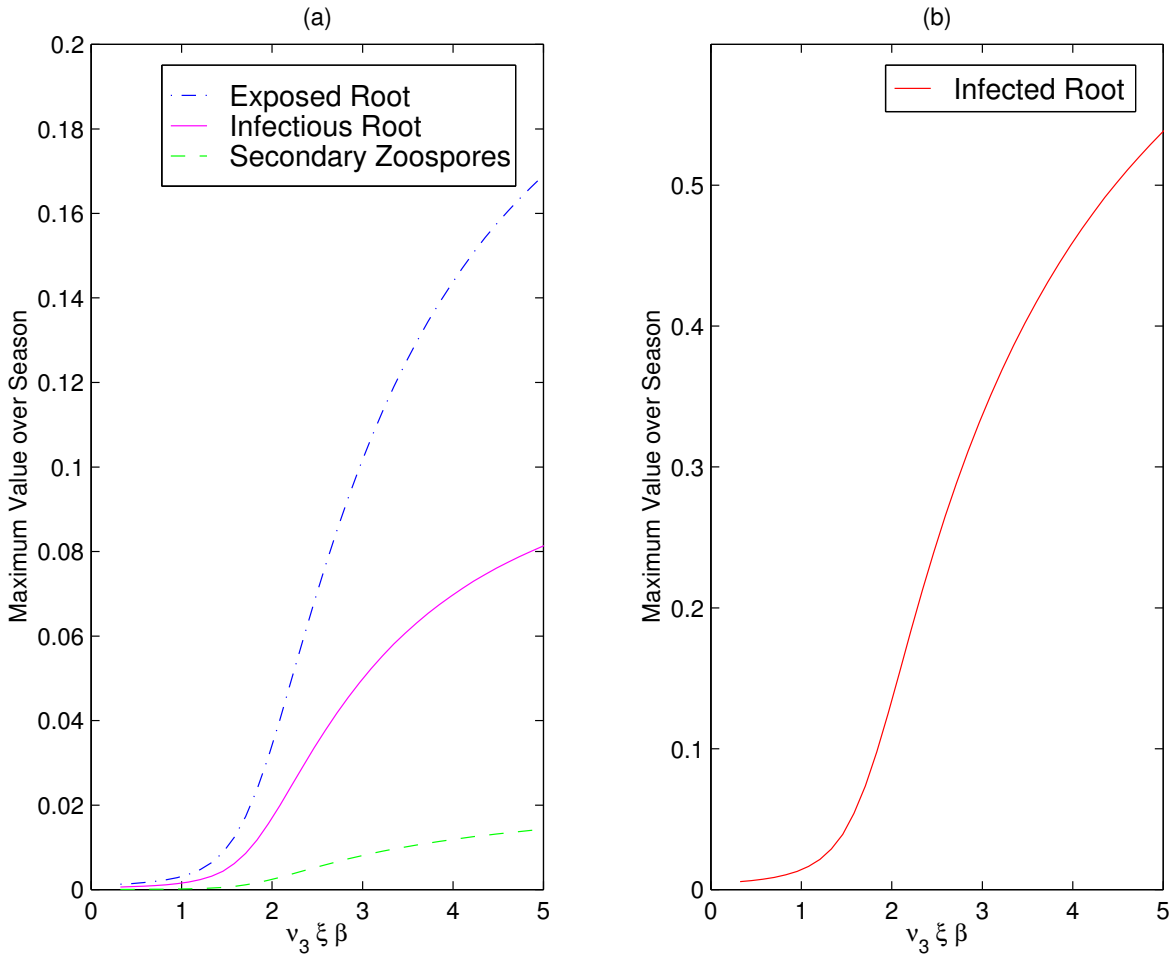

Figure 3.7: Variation of the maximum value of x, c, c_p and z, given monomolecular growth of n, as a function of $\nu_3\xi\beta$ as ϵ_2 is varied, with other parameters as in Figure 3.4. It can be seen that there is a transition form primary infection (low values of z) to secondary infection (higher values of z) as $\nu_3\xi\beta$ increases through order 1.

Chapter 4

Extending the Model

Two particular extensions to the model have been suggested by C.A. Gilligan (personal communication). These are the effect of varying temperatures on the progress of the disease, and introducing heterogeneous mixing terms for the interaction between the susceptible root and secondary zoospores. We discuss these extensions in Sections 4.1 and 4.2.

Also of interest, as discussed in Section 2.1.1, is the form of the growth function g. In section 4.3, we investigate the system with a small constant growth rate.

4.1 Temperature Variation

In this section, we examine the effects of temperature on the parameters of our model, and hence on the dynamics of the infection. Experimental results are used to motivate the choice of the form of the parameter variation, and this is then included in the model. This model is then used, under certain restrictions, to discuss the effect of different temperatures on the development of the disease.

4.1.1 Experimental Results

The effects of temperature on the infection of sugar beet by *Polymyxa betae* was investigated by Blunt *et al* [4] in 1991. Sugar beet seedlings were grown in infected soil at fixed temperatures and examined at various time periods to investigate what proportion of the roots of the plants were infected. Three experimental conditions were included at each of five temperatures: *P. betae* infected seedlings were planted in *P. betae*-free soil and uninfected seedlings were planted in infected and uninfected soil. Samples of each were placed randomly in separate growth cabinets at temperatures of 10°C, 15°C, 20°C, 25°C and 30°C.

The sugar-beet seedlings were sampled daily. At each sampling, five replicate plants were randomly selected from an experiment at each temperature. These were

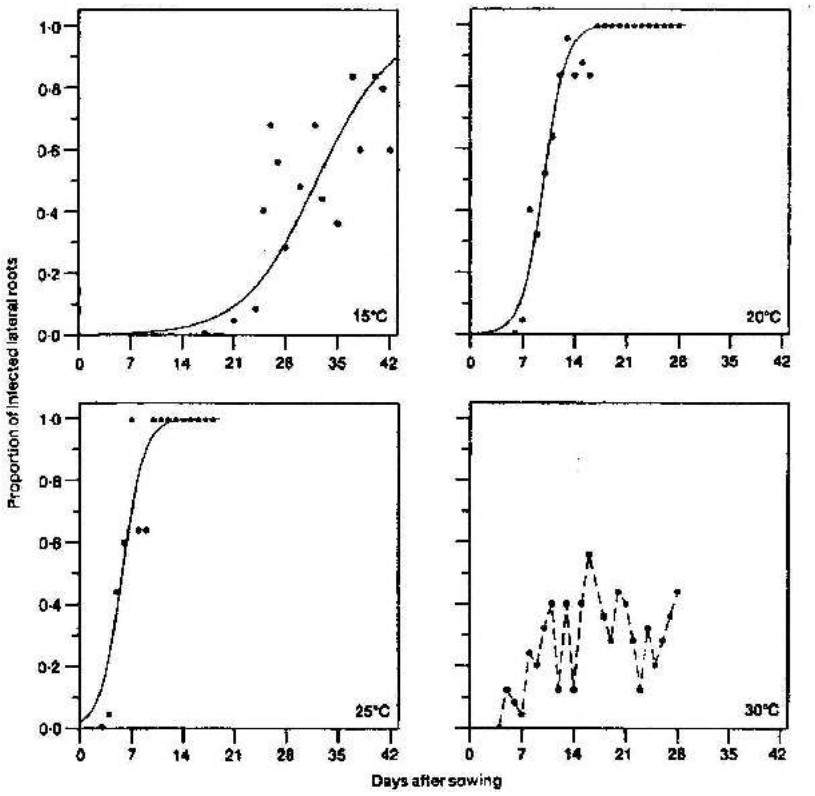

Figure 4.1: Results from experiments. Reproduced from [4].

cleaned, and the oldest lateral roots from every seedling were examined for signs of infection, using a microscope. If there was evidence of any part of the life cycle of the fungus, zoospores, plasmodia or cystori, then that section of root was considered to be infected. The proportion of the root which was infected was noted.

The proportion of root which had been exposed to the infection, Y, was plotted against time. A logistic curve of the form

$$Y = \frac{K_u}{1 + \exp(-\beta(t - \delta))}, \tag{4.1}$$

was fitted to the data. The results are shown in Figure 4.1. There was no evidence of infection at 10°C. The experiment at 30°C gave results to which a logistic curve could not be fitted. The parameters of these logistic curves are given in Table 4.1. The effect of temperature on β and δ is dramatic, over only a ten degree range.

From these results Blunt *et al* deduce that as the temperature increases from 15°C to 25°C the delay before infection decreases. The rate of fungal development increases over this range of temperatures. At 30°C the primary infection is rapid, but the subsequent development of the fungi is erratic and restricted.

The general biological conclusions that Blunt *et al* make from their results on the effect of temperature on infection of sugar beet seedlings by *Polymyxa betae* are in

Parameter	15°C	20°C	25°C
Rate (β days^{-1})	0.203±0.035	0.677±0.089	0.677±0.089
Delay (δ days)	32.27±1.55	9.87±0.21	5.78±0.39
Asymptote(K_u)	1.00	1.00	0.677±1.00

Table 4.1: Estimates of the parameter in a logistic model of the form (4.1), for the proportion of fibrous roots of sugar-beet seedlings infected by *Polymyxa betae* at three temperatures. The parameter K_u was fixed. Reproduced from Table 1 in [4].

two main areas. There was an effect on the time before infection was initiated, this time was shortest at 25°C. The second effect, on the development of the fungi, was less clearly defined. The results showed the same rate of development of the logistic model at 20 and 25°C. The observed time for an initial infection to develop into a mature cystorus was 9 days at 15°C, 6 days at 20 and 25°C and 15 days at 30°C. Thus, plants growing in infected soil became infected most rapidly at 25°C.

The results from the experiments at 30°C did not give a clear increase or decrease in infection rates from 25°C. This is perhaps due to an effect on the development of the sugar beet seedlings, as well as the fungus, at such a high temperature. No infection was observed at 10°C within 80 days of planting, which suggests that there is a threshold for infection between 10 and 15°C.

For the purposes of the inclusion of the effect of temperature variation in our model, we note that infection rates and the development time of the fungi increase between 10 and 25°C.

4.1.2 Including Temperature Variation in the Model

While we cannot relate the parameter variations in this paper directly to the parameters in our model, we can use the biological conclusions to motivate certain parametric variations with temperature. It should be noted that on solving our model (with logistic, exponential or constant growth term) the proportion of the root that has been infected plots an exponential, not a logistic, curve. Thus no direct comparison can be made. It should also be noted that the experiments concentrate on only the first lateral root formed, while our model considers the whole fibrous root system.

In order to use these experimental results, we must consider the biological deductions made in this paper. Our model does not include a delay time before the infection begins, so this effect cannot be related to the model. The time taken for the plasmodia to develop, however, is included in the form of the delay parameters β_1 and β_2. We recall that $\beta_{1,2}^{-1}$ is the 'average latent period prior to release of secondary (primary) zoospores'. Thus if we were to assume, from the experimental results that as the temperature increases this time decreased, then $\beta_{1,2}$ increase. The parameter

$\beta_1 = 0.5$ and is assumed to be the value at 25°C.

We shall restrict our consideration to the temperature range $12 - 25$°C (assuming that the fungus becomes active at 12°C).

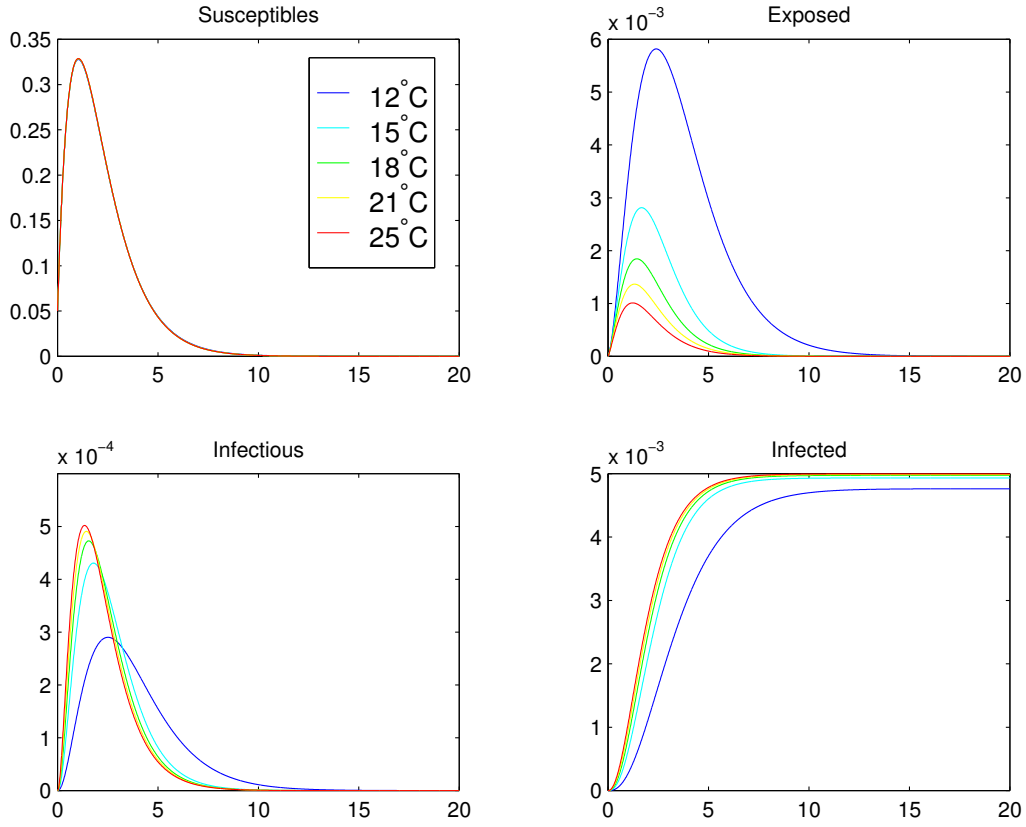

Figure 4.2: Numerical solutions to the temperature dependent model at constant temperature. Parameters as in [16].

For simplicity, we assume that the variations of $\beta_{1,2}$ are linearly increasing with temperature. Our parameter values are taken to be at 25°C, so this will be the maximum value of the parameters. From Table 2.1 we can see that $\beta_1 = 0.5$, and so we shall take this down to about 0.2 at 15°C, a fall of about 60%. The parameter $\beta_2 = 0.2$ at 25°C, which we reduce by about 60% to 0.12 at 15°C.

As the temperature increases, the number of susceptibles remains the same. As $\beta_{1,2}$ increases with temperature, $\beta_{1,2}^{-1}$ decreases, thus the time that zoospores spend forming plasmodia is decreased, and so the number of exposed roots will be less. The overall infection should be more vigorous however, since secondary zoospores are being formed more quickly. Thus the levels of infectious and infected root should be larger as the temperature increases. In secondary infections, the effect should be more noticeable, since it is the speed of production of the secondary zoospores which has immediate impact on the dynamics. The effect of these parameter variations at constant temperature are shown in Figure 4.2, in the typical parameter range, and

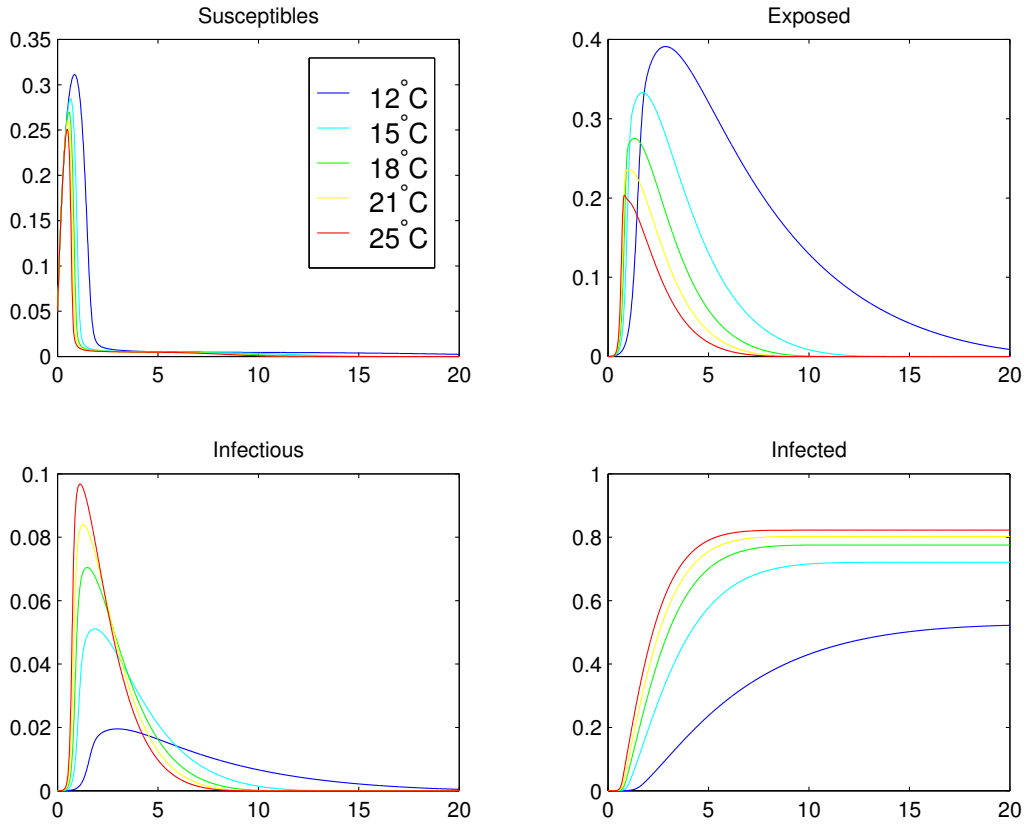

Figure 4.3: Constant temperature solutions to the equations. Parameters as in [16], except ϵ_2 which has been multiplied by 100 to bring the dynamics into a secondary infection.

Figure 4.3 shows the results with larger ϵ_2, with the secondary infection dominant.

4.1.2.1 Variable Temperature

We now consider the effect on our model of varying the temperature throughout the season, comparing the effects in different countries, and for different times of planting. Figure 4.4 shows the average daily temperature in Cambridge and Rome. The data comes from *http:/www.worldclimate.com*, who have used several official sources. Cambridge has been chosen because it is near to IACR Broom's Barn, where the experiments were carried out for [3]. Rome has been chosen as an example of typical temperatures in Italy, where there are far higher incidences of rhizomania.

We shall approximate the variation of temperature during a planting season by a sine curve, and compare typical curves for England and Italy, based on Figure 4.4. The higher temperatures throughout the year in Italy should lead to higher levels of infection, while the rise in temperatures towards the second half of the season may lead to a second phase of infection, provided that all the susceptible roots have not been removed. The results from numerical simulations are shown in Figure 4.5. There is little difference in the amount of infection, so our model does not explain

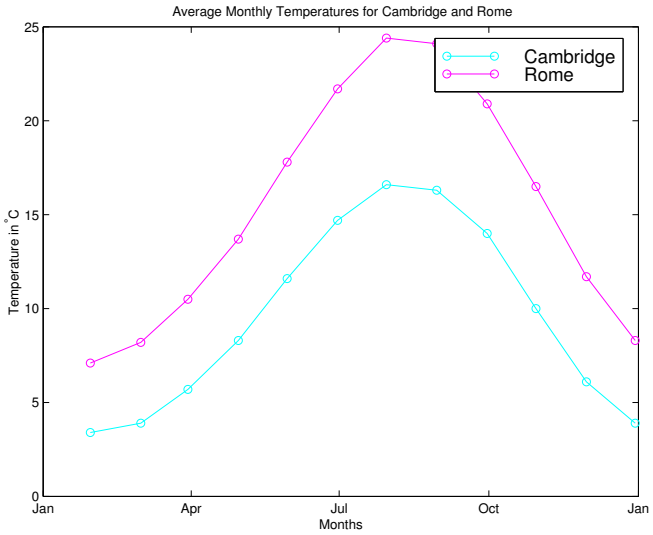

Figure 4.4: Average monthly temperatures in Cambridge and Rome.

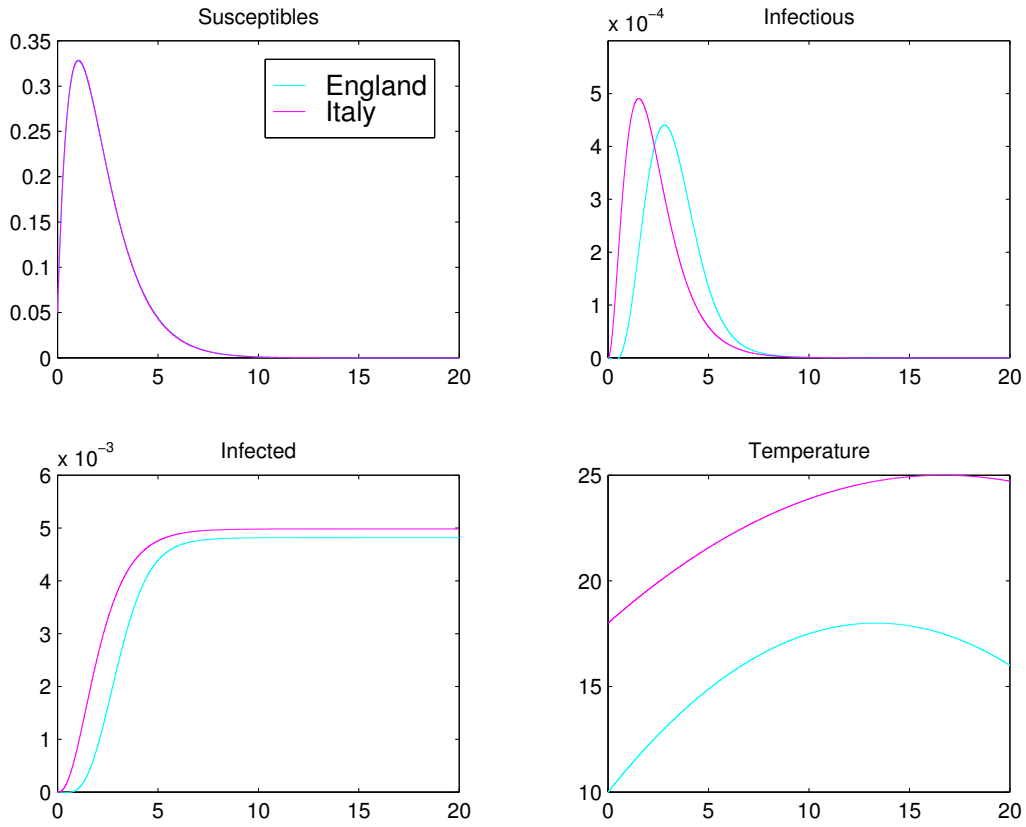

Figure 4.5: Comparing results from approximating temperature variation in England and Italy.

this phenomenon.

4.2 Heterogeneous Mixing

Heterogeneous mixing terms may be a more suitable way of modelling the interaction between the susceptible root and the secondary zoospores than the sz term used in our model. The secondary zoospores are produced at the root and so are highly dependent on the density of root for the success of reinfection. This may mean that the interaction with the susceptible could be modelled more effectively with a different mathematical form. In this section, we shall discuss the effect of introducing quadratic and cubic interactions. This means that the probability of a secondary zoospore infecting a root dies off more quickly as the density of root decreases. We would not expect this new term to have an effect in the parameter regions where the secondary infection is not playing an important role. Our analysis would be almost identical to that in Section 3.3, although our parameter values would be different. In the case where the secondary infection is more important, this may have an effect. We shall investigate mixing terms of the form $s^a z^a$ where $a = 2, 3$.

Our heterogeneous mixing model is

$$\begin{aligned}
\text{Total:} \quad \frac{dN}{dt} &= rN\left(1-\frac{N}{K}\right) = G(t), && (4.2)\\
\text{Susceptibles:} \quad \frac{dS}{dt} &= G(t) - \lambda_1 SP - \lambda_a S^a Z^a - mS + \sigma I_Z, && (4.3)\\
\text{Exposed:} \quad \frac{dE}{dt} &= \lambda_1 SP + \lambda_a S^a Z^a - \beta_1 E - \beta_2 E, && (4.4)\\
\text{Infectious:} \quad \frac{dI_Z}{dt} &= \beta_1 E - \sigma I_Z, && (4.5)\\
\text{Infected:} \quad \frac{dI_P}{dt} &= \beta_2 E, && (4.6)\\
\text{Resistant:} \quad \frac{dR}{dt} &= mS, && (4.7)\\
\text{Secondary Zoospores:} \quad \frac{dZ}{dt} &= \gamma I_Z - \eta_a S^a Z^a - \alpha Z, && (4.8)\\
\text{Primary Zoospores:} \quad \frac{dP}{dt} &= -\epsilon P, && (4.9)
\end{aligned}$$

where the parameters and variables are as before, except λ_a and η_a, which will have to change with the index a. We have no data to support a particular choice of parameters λ_a and η_a.

If we rescale the equations, as in Chapter 3, the first rescaling is the same as (3.3) to (3.10), except for the modified terms. The main equations are

$$\text{Susceptibles:} \quad \frac{ds}{d\tau} = g(\tau) - \epsilon_1 sp - \epsilon_a s^a z^a - s + \kappa c, \qquad (4.10)$$

$$\text{Exposed:} \quad \frac{dx}{d\tau} = \epsilon_1 sp + \epsilon_a s^a z^a - b_3 x, \tag{4.11}$$

$$\text{Infectious:} \quad \frac{dc}{d\tau} = b_1 x - \kappa c, \tag{4.12}$$

$$\text{Secondary Zoospores:} \quad \frac{dz}{d\tau} = c - \theta_a s^a z^a - \xi z, \tag{4.13}$$

where

$$\theta_a = \frac{\eta_a K^{2a-1}\gamma^{a-1}}{m^{2a-1}}, \qquad \epsilon_a = \frac{\lambda_a K^{2a-1}\gamma^a}{m^{a+1}}. \tag{4.14}$$

In order to make these nondimensional parameters of a similar size to those in Chapter 3, we would need to choose $\eta_2 \approx 5 \times 10^{-7}$ days^{-1}cm^7, $\lambda_2 \approx 4 \times 10^{-8}$ days^{-1}cm^8, $\eta_3 \approx 6^{-11}$ days^{-1}cm^{13}and $\lambda_3 \approx 1 \times 10^{-14}$ days^{-1}cm^{14}. When we use these parameter values, the action of the secondary infection is so small as to be negligible, and this is a primary infection, similar to the results shown in Figure 3.4.

If we take ϵ_a and θ_a to be very large (order 10^7) we still only have primary infection occurring (c.f. Figure 3.4). This is probably because s does not become large enough to allow for secondary infection in the heterogeneous case.

4.3 Constant Growth Rate of Susceptible Root

As discussed in Section 2.1.1, a possible form for the growth rate, $g(t)$, of the susceptible root is a constant. This may be a more realistic representation of the growth rate if we consider the fact that the zoospores mainly infect the tips of the roots, which are growing at approximately a constant rate throughout the season [5]. We shall investigate the system with a constant growth rate $g \approx 1/20$, which is the ratio of the time taken for a susceptible root to become resistant to the length of the season.

In the main, the analysis of Chapter 3 does not depend on the form of g, except when the analytical solutions are calculated. In fact, $\bar{g}$ is now approximately 0.01 throughout the season, and so the analysis which relies on g being small is valid.

Since g does not decrease towards zero over time, as it does in the examples in Chapter 3, s will not decrease towards zero, but, as we can see from equation (3.4), increases towards g. This means that there is a non-zero steady state of the equations (3.4), (3.5), (3.6) and (3.9). The steady state values of z_1, c_1, s_1 and x_1 satisfy

$$\begin{aligned} 0 &= (\kappa\xi(b_3\epsilon_1 + b_2\epsilon_2))z_1^2 \\ &\quad +(-b_1\epsilon_1\kappa\xi p - b_1\epsilon_2 g + b_3\xi + \kappa\theta b_3 g)z_1 - b_1\epsilon_1 gp \qquad (4.15) \\ c_1 &= z_1(\theta g + \xi\epsilon_1 z_1) + \frac{z_1}{\epsilon_1 z_1 + \epsilon_2 z_1 + 1 - \kappa\theta z_1} \qquad (4.16) \\ s_1 &= \frac{g + \kappa\xi z_1}{\epsilon_1 z_1 + \epsilon_2 z_1 + 1 - \kappa\theta z_1} \qquad (4.17) \\ x_1 &= \frac{\kappa}{b_1} z_1(\theta g + \xi\epsilon_1 z_1) + \frac{z_1}{\epsilon_1 z_1 + \epsilon_2 z_1 + 1 - \kappa\theta z_1} \qquad (4.18) \end{aligned}$$

respectively (Calculated in Maple V). Equation (4.15) has exactly one positive root, since the coefficient of z_1^2 is positive, and the constant term is negative. If ϵ_2 is large, then all these steady states are positive. Therefore, if we solve the equations for the same parameter values as Figures 3.4 to Figure 3.6, we would expect to see the solutions tending to this non-zero steady state when s has passed the threshold value in a secondary infection.

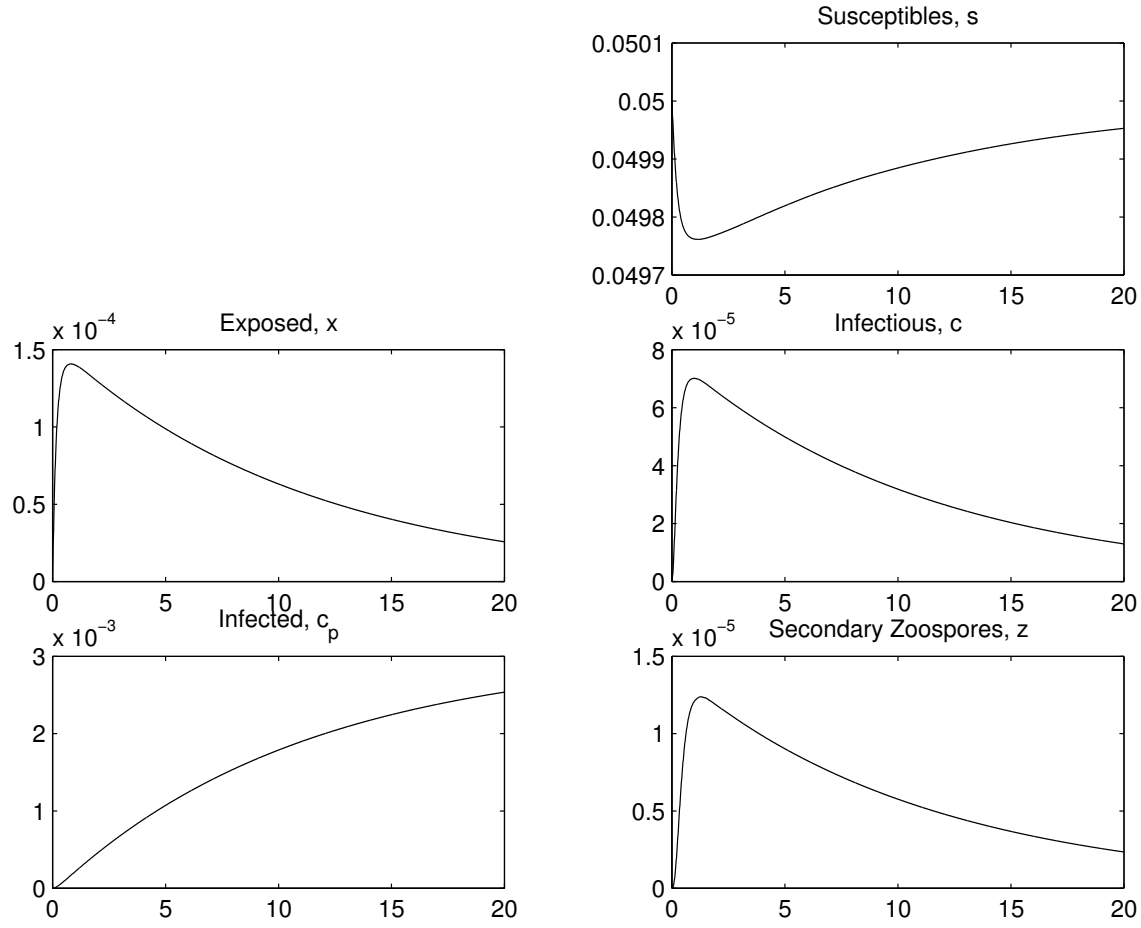

Figure 4.6: Numerical solutions of the system of equations (3.3) to (3.10), against time, τ, with the parameters as in Truscott *et al* (see Table 3.1). The condition $\nu_3\beta\xi < 1$ is satisfied, and the primary infection dominates. The variables x and c are of order $\epsilon_1 p_0$. (c.f. Figure 3.4)

In Figures 4.6 and 4.7 we can see that s varies only slightly before going to its equilibrium value, of approximately g, while all the other variables remain small. However, in Figure 4.8, there is a noticeable change in the form of the solutions, with the variables going to a non-zero steady state. While z, c and x remain small, $\dot{s} \approx g - s$ which has a steady state at g, which is the steady state in the first two graphs. If however, these variables become large, the steady state of s decreases, as in Figure 4.8. This marked change in the solutions would occur in a continuous manner

as $\nu 3\beta\xi$ varied.

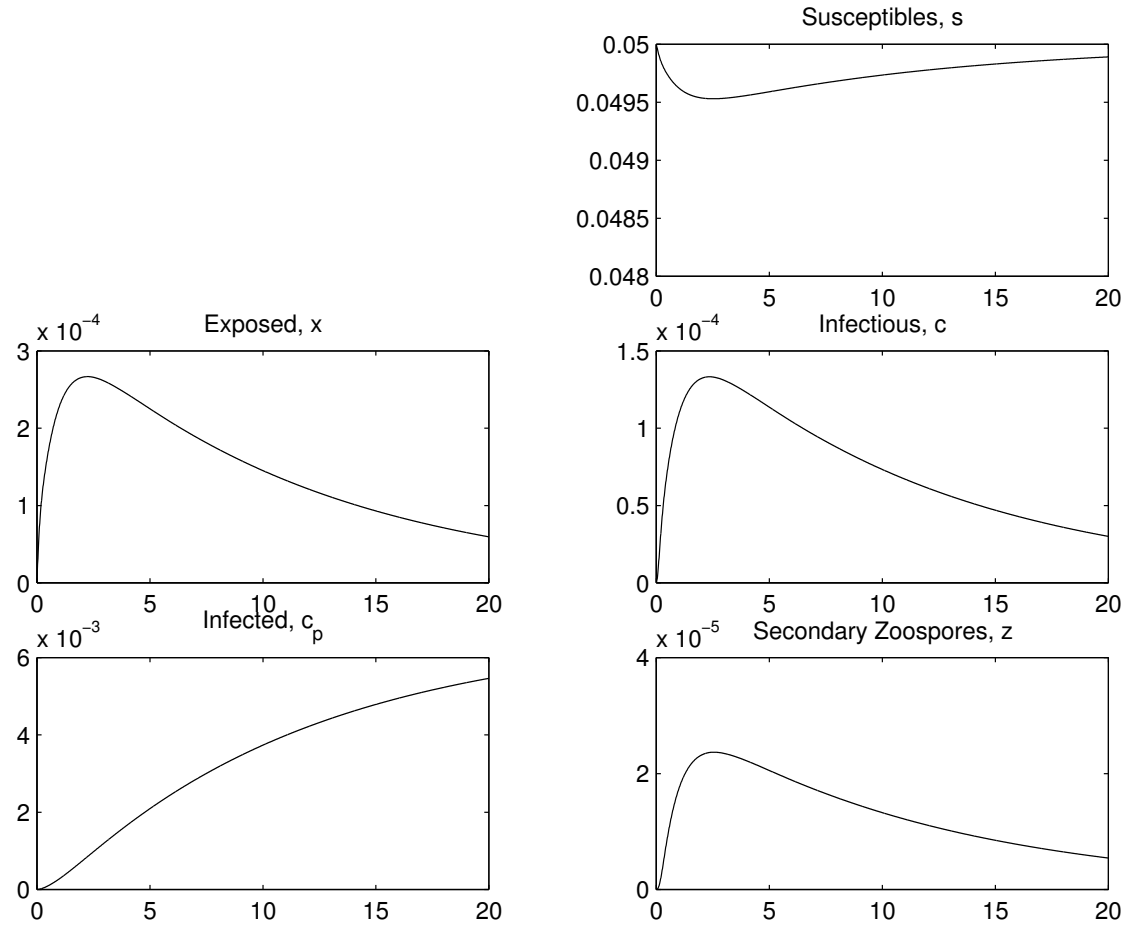

Figure 4.7: Numerical solutions of the system of equations (3.3) to (3.10), against time, τ, with the parameters as in Truscott *et al* (see Table 3.1). The condition $\nu_3\beta\xi > 1$ is satisfied, but s remains less than the threshold value of 0.5. The variables x and c are of order $b_3\xi/\theta$. (c.f. Figure 3.5)

Using these steady states, we can approximate the amount of infected root, c_p left at the end of a season as

$$c_p(\infty) \approx b_1 \int_0^{20} x d\tau \tag{4.19}$$

$$\approx 20 b_1 x_s. \tag{4.20}$$

Thus, a condition on the parameters for the infection to 'bulk up' or 'fade out' could be approximated, as in Chapter 3.

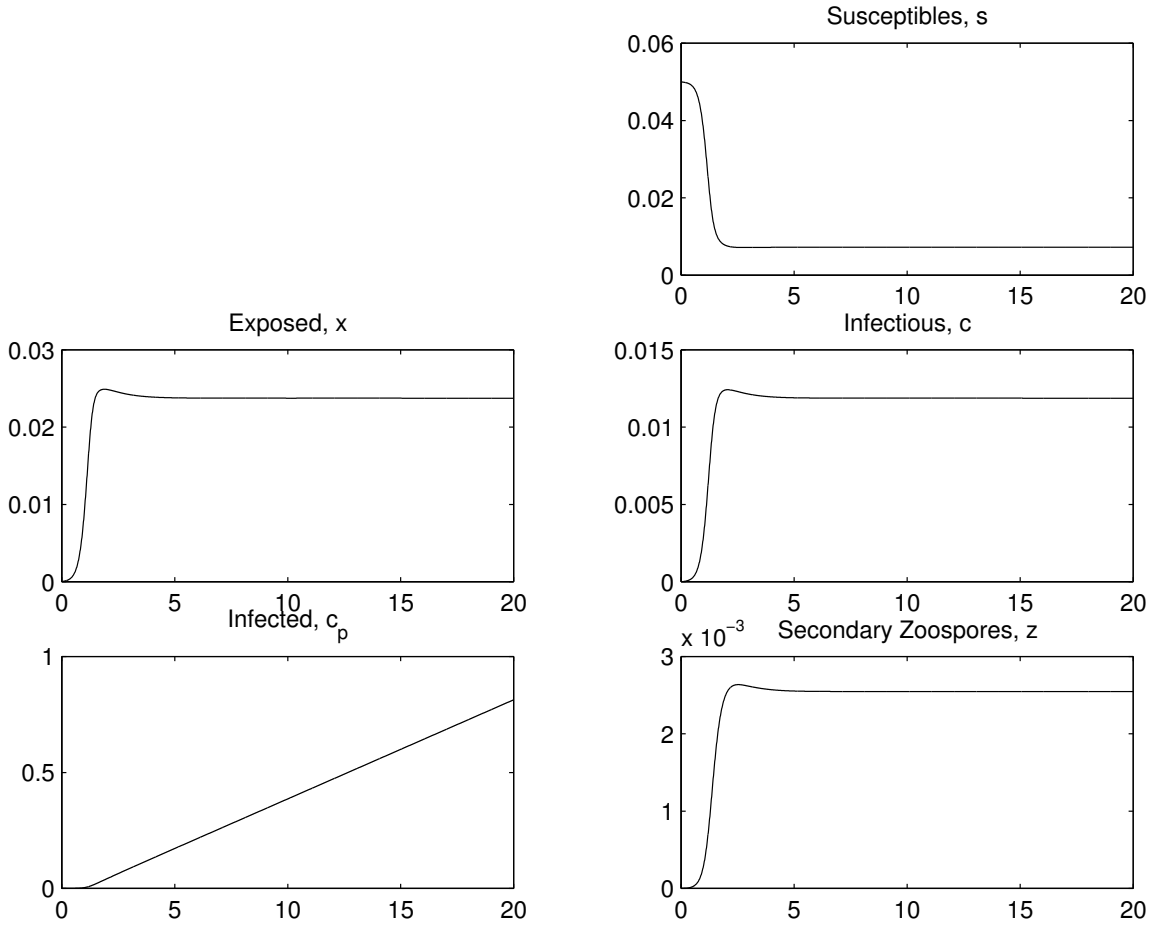

Figure 4.8: Numerical solutions of the system of equations (3.3) to (3.10), against time, τ, with the parameters as in Truscott *et al* (see Table 3.1), except ϵ_2, which is multiplied by 100. The condition $\nu_3\beta\xi > 1$ is satisfied, and s is greater than the threshold value, giving secondary infection. The variables x and c are of order $\epsilon_1 p_0$. (c.f. Figure 3.6)

Chapter 5

Conclusions

In Chapter 1 of this dissertation we described the biology of the interaction between the fungus *Polymyxa betae* and the fibrous roots of *Beta vulgaris*, or sugar beet, which we then modelled mathematically. A compartmental model, derived in Truscott *et al* [16], was presented in Chapter 2. The parameter values in this model were examined and possible inconsistencies in some of these parameters were identified, namely in the choice of λ_2 and η (and the nondimensional variable θ in Chapter 3).

This model was then analysed in Chapter 3, in order to derive conditions under which a primary or secondary infection could occur. The primary infection is essentially caused by the pre-existing zoospores in the soil. The secondary infection is characterised by the bulk of the infection being due to reinfection by zoospores released from sporangial plasmodia in the roots. A possible measure of the relative efficacy of the primary and secondary infections is $\lambda_2 Z_{\max}/\lambda_1 P(0)$. When this is nondimensionalised, it becomes $(\epsilon_2/\epsilon_1)z_{max}$. In the figures where we have indicated that there is a secondary infection, this is larger than in the cases where there is a primary infection. The analysis showed that if

$$\frac{\lambda_2\gamma\beta_1}{\eta\sigma(\beta_1+\beta_2)} > 1, \tag{5.1}$$

and the density of susceptible root, S satisfies

$$S > K\left(\frac{\lambda_2\gamma\beta_1}{\eta\sigma(\beta_1+\beta_2)} - 1\right)^{-1}, \tag{5.2}$$

in terms of the original variables of the model, then a secondary infection would occur. This was demonstrated for particular parameter values in Section 3.4. The parameter values which are used in Truscott *et al* are not rigorously defined, due to a lack off experimental data, and so these parameters may vary, possibly by large amounts. In this case one of the conditions above may be satisfied, leading to secondary infection. Biologically, these conditions correspond to an increased rate of infection per secondary zoospore, λ_2, rate of release of these zoospores, γ, and average period over

which the roots are infectious, σ^{-1}. They also correspond to an increase in the length of root infected by a single zoospore λ_2/η. The condition on S means that there must be a sufficiently large amount of susceptible root available for infection. These conditions are intuitively consistent with the biology of this disease. The derivation of a condition for which the infection will build up from season to season, or die out, is outlined at the end of Chapter 3, along with a condition on the parameters for such behaviour.

Some modification and extensions to the model were investigated in Chapter 4. The first was the effect of temperature on the infection. Experimental results [4] show that there are dramatic effects on the infection as temperature varies. The parameters which caused these effects were identified and allowed to vary with temperature in the model. The variation in these parameters led to switching between primary and secondary infection as the temperature increased, for particular parameter sets. Thus the model was successfully extended to include the effect of various constant temperatures throughout the season. The application of this extended model to an example of variable temperature gave sensible results, but on its own, failed to give an explanation for the difference between infection levels in England and Italy. This difference may be because the disease has been present in Italy for many years, while in England it has only become a problem recently, and preventative measures, such as cleaning seed, have been used to try and combat the disease.

The inclusion of heterogeneous mixing terms, in Section 4.2, was designed as a possible way to model the fact that if there is less susceptible material present, the secondary zoospores have a much lower chance of infecting a portion of root. This was expected to reduce the occurrences of secondary infection, and in fact no examples of secondary infection could be found. This is probably due to the fact that the susceptible variable does not become large in a primary infection, and so the secondary zoospores were infecting low amounts of susceptible material.

The growth rate of the fibrous root is possibly unrealistic in the original model. It is the tips of the roots which are susceptible, and if, as an idealisation, these are growing outwards at a constant rate, then the growth rate should be constant. In Section 4.3 this form of growth rate was studied. The numerical solutions behaved in much the same way as the original model, except when there was a secondary infection. In this case the system went to a non-negative steady state, leading to approximately linear growth of the infected material. In this case, the infection in the following season will be greatly increased.

There are many further areas in which this model could be extended and modified. A primary area for further research would be consideration of whether it is realistic to model a spatially varying system by a homogeneous model, since clearly spatial variation is important on both a macro and micro scale.

Appendix A

Glossary of Terms

This glossary contains some of the biological terms used in this dissertation. The definitions are adapted from entries in [9] and [10]

endogenous - (1) living inside, (2) immersed in substrate, (3) undergoing development within.

flagella(sing. flagellum) - an appendage of a motile cell, sometimes of taxonomic significance. In fungi two types can be distinguished: whiplash, with a smooth continuous surface covered with processes like hairs, the mastigonemes or flimmers. In bacteria the cell may have flagella arising from any part of the wall, i.e. it is petrichous; or from one end, one or several, i.e. it is polar or cephalotrichous; see *zoospore*.

obligate parasite - an organism that occurs in an intimate association with, and which is wholly dependent for its nutrition on, another living organism; parasite, parasitism, applies to a mode of existence, pathogen which see to causing disease; obligate is the antonym of facultative.

plasmodium(pl. plasmodia) - a multinucleate, motile mass of protoplasm bounded by a plasma membrane but lacking a wall, generally *reticulate*, characteristic of the growth phase.

reticulate- like a net, netted.

sporangiospore - walled spore produced in a sporangium; primary infestation, 1-4 nucleate, thick-walled spore which serves to transmit an infestation from one host individual to another; secondary infection; multinucleate, thin-walled spore which germinates in the same gut as they were produced.

zoospore - A unicellular propagating or disseminating body with one or two *flagella*, and having limited mobility.

References

[1] M.J.C. Asher. Rhizomania. In D.A. Cooke and R.K. Scott, editors, *The Sugar Beet Crop: Science into Practice*. Chapman and Hall, 1993.

[2] IACR-Broom's Barn. http://www.iacr.bbsrc.ac.uk/res/depts/broom/tresearch.html. World Wide Web Pages.

[3] S.J. Blunt. *The ecology of Polymyxa betae, a fungal root parasite of Beta vulgaris*. PhD thesis, University of Cambridge, U.K., 1989.

[4] S.J. Blunt, M.J.C. Asher, and C.A. Gilligan. Infection of sugar beet by *Polymyxa betae* in relation to soil temperature. *Plant Pathology*, 41:148–53, 1991.

[5] K.F Brown and P.V. Biscoe. Fibrous root growth and water use of sugar beet. *Journal of Agricultural Science*, 105:679–691, 1985.

[6] J.S. Gerik, J.C. Hubbard, and J.E. Duffus. Soil matric potential effects on infection by *Polymyxa betae* and bynvv. *Proceedings of the First Symposium of the International Working Group on Plant Viruses with Fungal Vectors, Braunshweig, Eugen-Ulmer, Stuttgart*, pages 75–78, 1990.

[7] C.A. Gilligan and A. Kleczkowski. Population dynamics of botanical epidemics involving primary and secondary infection. *Philosophical Transactions of the Royal Society, London, Series B*, 352:591–608, 1997.

[8] D. Hanselman and B. Littlefield. *Mastering Matlab 5, A Comprehensive Tutorial and Reference*. The MathWorks, Inc, 1998.

[9] D.L. Hawksworth, P.M. Kirk, B.C. Sutton, and D.N. Pegler. *Ainsworth and Bisby's Dictionary of the Fungi*. CAB International, 1995.

[10] P. Holliday. *A Dictionary of Plant Pathology, 2nd Edition*. Cambridge University Press, 1998.

[11] B. Keskin. *Polymyxa betae*, ein Parasit in den Wurzeln von *Beta vulgaris* Tournefort, besonders während der Jugendtwicklung de Zukerrübe. *Archiv für Mikrobiologie*, 49:348–374, 1964.

[12] University of Ohio. http://www.plantbio.ohiou.edu/pbc/plasmos/. World Wide Web Pages.

[13] D. Peters and A. Godfrey-Veltman. Inoculum characteristics of zoospore suspensions of *Polymyxa betae* infected with beet necrotic yellow vein virus. *Proceedings of the First Symposium of the International Working Group on Plant Viruses with Fungal Vectors, Bruanschweig, Eugen Ulmer, Stuttgart*, pages 69–73, 1990. TBR.

[14] M. Richard-Molard. Rhizomania: A world-wide danger to sugar-beet. *Span*, 28:92–4, 1985.

[15] British Sugar. http://www.britishsugar.co.uk/bsweb/bshome.htm. World Wide Web Pages.

[16] J.E. Truscott, C.R. Webb, and C.A. Gilligan. Asymptotic analysis of an epidemic model with primary and secondary infection. *Bulletin of Mathematical Biology*, 59(6):1101–1123, 1997.

[17] G. Tuitert. Assessment of the inoculum potential of *Polymyxa betae* and beet necrotic yellow vein virus (bynvv) in soil using the most probably number method. *Netherlands Journal of Plant Pathology*, 96:331–41, 1990.

[18] G Tuitert and G.J. Bollen. Recovery of resting spores of paolymyxa beatae from soil and the influence of duration of the bioassy on the detection level of beet necrotic yellow vein virus in soil. *Netherlands Journal of Plant Pathology*, Supplement 3:219–230, 1993.

[19] G. Tuitert and Y. Hofmeester. Epidemiology of beet necrotic yellow vein virus in sugar beet at different initial inoculum levels in the presence or absence of irrigation: Dynamics of inculum. *Netherlands Journal of Plant Pathology*, 98:343–360, 1992.

[20] C.R. Webb, CA. Gilligan, and M.J.C. Asher. A model for the temporal buildup of *Polymyxa betae*. *Phytopathology*, 89(1):30–38, 1999.